Table 4 HR of regression from non-smoking CIN1/2 according to the serum micronutrients and nutrient intake questionnaire

	n	Person-months	Events	Cumulative 2-year rate (95 % CI)	Hazard ratio for regression (95 % CI)			
					Unadjusted	*p* value	Adjusted model	*p* value
Serum retinol							*p* for trend	0.292
Low (<55.2)	62	809.8	39	67.0 (54.5–79.0)	1		1	
Medium (55.2–67.9)	70	922.3	41	62.8 (50.9–74.6)	0.93 (0.60–1.44)	0.75	1.03 (0.65–1.63)	0.908
High (>67.9)	58	743.4	39	71.4 (58.7–83.1)	1.08 (0.69–1.68)	0.742	1.21 (0.74–1.98)	0.448
Serum α-carotene							*p* for trend	0.883
Low (<5.1)	46	560.7	28	64.4 (50.1–78.5)	1.00		1.00	
Medium (5.1–9.7)	62	789.7	38	66.1 (53.3–78.4)	0.97 (0.60–1.59)	0.918	1.22 (0.73–2.05)	0.449
High (>9.7)	82	1,125.1	53	68.7 (57.9–79.0)	0.93 (0.59–1.47)	0.76	1.26 (0.75–2.11)	0.384
Serum β-carotene							*p* for trend	0.206
Low (<28.3)	45	583.9	26	60.1 (45.8–74.7)	1.00		1.00	
Medium (28.3–57.6)	61	780.1	41	75.7 (62.7–86.9)	1.16 (0.71–1.90)	0.557	1.20 (0.71–2.03)	0.488
High (>57.6)	84	1,111.5	52	65.5 (54.8–76.0)	1.03 (0.64–1.65)	0.91	1.23 (0.73–2.07)	0.439
Serum zeaxanthin/lutein							*p* for trend	0.024
Low (<42.9)	56	729.3	34	64.8 (51.4–77.8)	1.00		1.00	
Medium (42.9–57.3)	61	817.3	38	66.7 (54.2–78.9)	1.00 (0.63–1.59)	1	1.12 (0.69–1.84)	0.642
High (>57.3)	73	928.9	47	68.6 (57.1–79.5)	1.05 (0.68–1.64)	0.813	1.25 (0.78–2.01)	0.352
Serum cryptoxanthin							*p* for trend	0.129
Low (<11.2)	47	650.1	28	64.7 (50.0–79.1)	1.00		1.00	
Medium (11.2–22.1)	61	740.7	38	68.2 (55.3–80.4)	1.23 (0.75–2.00)	0.414	1.24 (0.74–2.08)	0.412
High (>22.1)	82	1,084.7	53	67.5 (56.8–77.8)	1.16 (0.73–1.83)	0.536	1.35 (0.82–2.22)	0.231
Serum lycopene							*p* for trend	0.269
Low (<19.8)	63	805.3	37	63.2 (50.7–75.7)	1.00		1.00	
Medium (19.8–35.8)	63	827.7	43	73.8 (61.5–84.8)	1.11 (0.71–1.72)	0.651	1.17 (0.73–1.87)	0.51
High (>35.8)	64	842.5	39	64.3 (52.0–76.4)	1.00 (0.63–1.55)	0.962	1.28 (0.79–2.07)	0.316
Serum α-tocopherol							*p* for trend	0.176
Low (<753.0)	60	731.7	39	67.1 (54.7–79.0)	1.00		1.00	
Medium (753.0–983.9)	63	829.9	40	67.5 (55.2–79.2)	0.91 (0.59–1.42)	0.676	0.96 (0.60–1.53)	0.866
High (>983.9)	67	913.9	40	66.5 (53.9–78.6)	0.81 (0.52–1.26)	0.344	0.96 (0.60–1.54)	0.859
Retinol intake							*p* for trend	0.892
Low (<190.2)	62	760.7	36	63.5 (50.5–76.4)	1.00		1.00	
Medium (190.2–313.1)	63	840.7	41	70.4 (57.9–82.0)	1.04 (0.67–1.63)	0.854	0.90 (0.53–1.54)	0.704
High (>313.1)	65	874.1	42	66.3 (54.5–77.7)	1.02 (0.65–1.59)	0.94	0.86 (0.48–1.53)	0.61
Carotene intake							*p* for trend	0.131
Low (<3,281.4)	47	606.4	29	67.7 (52.7–81.9)	1.00		1.00	
Medium (3,281.4–5,042.8)	71	959.6	40	62.1 (50.0–74.2)	0.88 (0.55–1.43)	0.615	0.89 (0.51–1.56)	0.676
High (>5,042.8)	72	909.5	50	70.8 (59.8–81.0)	1.16 (0.74–1.84)	0.515	1.08 (0.60–1.94)	0.804
Vitamin A intake							*p* for trend	0.134
Low (<2,398.8)	50	676.0	28	63.5 (48.8–78.2)	1.00		1.00	
Medium (2,398.8–3,466.7)	69	934.1	41	63.8 (51.7–75.8)	1.08 (0.67–1.75)	0.755	1.14 (0.65–1.99)	0.654
High (>3,466.7)	71	865.4	50	72.3 (61.3–82.4)	1.42 (0.89–2.25)	0.14	1.47 (0.79–2.73)	0.218
Vitamin E intake							*p* for trend	0.163
Low (<6.7)	51	631.5	29	61.3 (47.4–75.5)	1.00		1.00	
Medium (6.7–8.7)	62	884.3	39	66.0 (53.6–78.1)	0.98 (0.61–1.58)	0.932	1.38 (0.70–2.71)	0.354
High (>8.7)	77	959.7	51	70.3 (59.3–80.6)	1.16 (0.74–1.83)	0.519	1.44 (0.67–3.12)	0.352

Cox's proportional hazard model showing the hazard ratio for regression in a cumulative 24-month period in non-smokers. The adjusted model was identical to the model used in Table . The units of micronutrients are expressed as μg/dL

Table 5 HR of regression from current smoking CIN1/2 according to the serum micronutrients and nutrient intake questionnaire

	n	Person-months	Events	Cumulative 2-year rate (95 % CI)	Hazard ratio for regression (95 % CI)			
					Unadjusted	*p* value	Adjusted model	*p* value
Serum retinol							*p* for trend	0.43
Low (<55.2)	47	614.0	27	64.0 (49.2–78.6)	1		1	
Medium (55.2–67.9)	38	417.6	24	70.5 (53.4–85.7)	1.29 (0.74–2.23)	0.369	1.54 (0.87–2.76)	0.141
High (>67.9)	57	780.5	21	42.9 (30.1–58.3)	0.60 (0.34–1.06)	0.08	0.54 (0.29–1.00)	0.05
Serum α-carotene							*p* for trend	0.898
Low (<5.1)	59	751.9	33	62.5 (49.2–75.8)	1.00		1.00	
Medium (5.1–9.7)	53	689.6	22	49.9 (35.3–66.7)	0.72 (0.42–1.24)	0.24	0.85 (0.48–1.53)	0.595
High (>9.7)	30	370.6	17	61.8 (43.6–80.2)	1.04 (0.58–1.87)	0.886	1.23 (0.63–2.39)	0.537
Serum β-carotene							*p* for trend	0.667
Low (<28.3)	63	788.0	31	58.1 (44.6–72.2)	1.00		1.00	
Medium (28.3–57.6)	53	700.2	27	54.5 (41.1–69.1)	1.02 (0.61–1.71)	0.94	1.07 (0.62–1.86)	0.808
High (>57.6)	26	323.9	14	66.6 (44.5–87.0)	1.06 (0.56–2.00)	0.854	1.04 (0.51–2.14)	0.915
Serum zeaxanthin/lutein							*p* for trend	0.373
Low (<42.9)	54	640.8	32	63.6 (50.0–77.0)	1.00		1.00	
Medium (42.9–57.3)	52	669.4	26	54.1 (40.4–69.0)	0.79 (0.47–1.33)	0.372	0.88 (0.51–1.52)	0.645
High (>57.3)	36	501.9	14	57.6 (37.9–78.8)	0.55 (0.29–1.02)	0.059	0.76 (0.37–1.53)	0.435
Serum cryptoxanthin							*p* for trend	0.866
Low (<11.2)	62	727.3	36	67.4 (53.9–80.2)	1.00		1.00	
Medium (11.2–22.1)	47	644.3	20	48.4 (33.9–65.2)	0.63 (0.36–1.09)	0.098	0.72 (0.39–1.31)	0.279
High (>22.1)	33	440.5	16	53.9 (36.6–73.1)	0.73 (0.40–1.31)	0.286	0.85 (0.44–1.64)	0.63
Serum lycopene							*p* for trend	0.517
Low (<19.8)	43	543.8	21	55.3 (39.9–71.9)	1.00		1.00	
Medium (19.8–35.8)	55	761.7	29	60.8 (46.7–75.1)	0.96 (0.55–1.69)	0.896	0.79 (0.42–1.48)	0.457
High (>35.8)	44	506.6	22	54.4 (39.2–70.9)	1.08 (0.59–1.96)	0.802	0.77 (0.38–1.54)	0.456
Serum α-tocopherol							*p* for trend	0.042
Low (<753.0)	53	594.2	34	68.8 (55.5–81.4)	1.00		1.00	
Medium (753.0–983.9)	49	718.2	19	43.5 (30.1–59.7)	0.47 (0.27–0.83)	0.009	0.53 (0.27–0.94)	0.03
High (>983.9)	40	499.7	19	66.7 (46.0–86.0)	0.64 (0.36–1.11)	0.114	0.76 (0.42–1.40)	0.383
Retinol intake							*p* for trend	0.58
Low (<190.2)	50	573.8	29	62.3 (48.3–76.4)	1.00		1.00	
Medium (190.2–313.1)	51	673.9	25	56.5 (42.1–71.9)	0.74 (0.43–1.26)	0.263	0.76 (0.42–1.37)	0.36
High (>313.1)	41	564.4	18	52.3 (36.2–70.6)	0.63 (0.35–1.13)	0.124	0.57 (0.29–1.13)	0.106
Carotene intake							*p* for trend	0.182
Low (<3,281.4)	64	730.7	34	59.8 (46.9–73.1)	1.00		1.00	
Medium (3,281.4–5,042.8)	43	632.0	22	58.7 (42.7–75.4)	0.72 (0.42–1.24)	0.238	0.71 (0.39–1.31)	0.272
High (>5,042.8)	35	449.4	16	52.9 (35.8–72.2)	0.73 (0.41–1.33)	0.309	0.55 (0.25–1.18)	0.122
Vitamin A intake							*p* for trend	0.268
Low (<2,398.8)	65	723.6	36	61.9 (49.1–74.9)	1.00		1.00	
Medium (2,398.8–3,466.7)	43	642.5	19	49.1 (34.4–66.2)	0.59 (0.34–1.03)	0.064	0.58 (0.31–1.07)	0.081
High (>3,466.7)	34	446.0	17	60.6 (42.2–79.4)	0.74 (0.42–1.32)	0.307	0.60 (0.28–1.32)	0.208
Vitamin E intake							*p* for trend	0.567
Low (<6.7)	61	684.0	32	56.7 (44.1–70.1)	1.00		1.00	
Medium (6.7–8.7)	45	720.6	19	49.0 (34.4–66.0)	0.56 (0.32–0.99)	0.047	0.51 (0.25–1.05)	0.066
High (>8.7)	36	407.5	21	67.3 (49.6–83.8)	1.02 (0.59–1.77)	0.947	0.56 (0.23–1.38)	0.211

Cox's proportional hazard model showing the hazard ratio for regression in a cumulative 24-month period in current smokers only. The adjusted model was identical to the model used in Table . The units of micronutrients are expressed as μg/dL

Table 6 HR of progression from entire CIN1/2 according to the serum micronutrients and nutrient intake questionnaire

	n	Person-months	Events	Cumulative 5-year rate (95 % CI)	Hazard ratio for progression (95 % CI)			
					Unadjusted	*p* value	Adjusted model	*p* value
Serum retinol							*p* for trend	0.372
Low (<55.2)	128	4,588.2	7	8.7 (3.6–20.1)	1.00		1.00	
Medium (55.2–67.9)	132	5,048.8	17	17.1 (10.8–26.6)	2.25 (0.93–5.44)	0.071	2.35 (0.95–5.77)	0.063
High (>67.9)	131	5,210.1	14	14.3 (8.5–23.7)	1.82 (0.73–4.51)	0.198	2.23 (0.88–5.60)	0.089
Serum α-carotene							*p* for trend	0.669
Low (<5.1)	127	4,506.6	13	15.4 (8.7–26.2)	1.00		1.00	
Medium (5.1–9.7)	133	4,955.5	17	16.0 (10.0–25.0)	1.21 (0.59–2.49)	0.609	1.08 (0.51–2.31)	0.835
High (>9.7)	131	5,385.0	8	9.6 (4.7–19.0)	0.52 (0.22–1.27)	0.153	0.46 (0.18–1.15)	0.098
Serum β-carotene							*p* for trend	0.337
Low (<28.3)	129	4,245.0	18	21.8 (13.6–33.9)	1.00		1.00	
Medium (28.3–57.6)	131	5,208.1	7	7.0 (3.2–14.7)	0.32 (0.13–0.77)	0.011	0.28 (0.11–0.71)	0.007
High (>57.6)	131	5,394.0	13	13.2 (7.7–22.3)	0.58 (0.28–1.19)	0.14	0.52 (0.24–1.13)	0.098
Serum zeaxanthin/lutein							*p* for trend	0.772
Low (<42.9)	130	4,611.4	11	12.1 (6.7–21.4)	1.00		1.00	
Medium (42.9–57.3)	130	5,291.5	17	17.9 (11.2–28.0)	1.37 (0.64–2.94)	0.415	1.58 (0.71–3.53)	0.266
High (>57.3)	131	4,944.2	10	9.4 (5.1–17.1)	0.87 (0.37–2.06)	0.756	0.95 (0.39–2.32)	0.908
Serum cryptoxanthin							*p* for trend	0.618
Low (<11.2)	129	4,591.6	12	12.2 (6.9–20.9)	1.00		1.00	
Medium (11.2–22.1)	130	4,906.2	16	17.1 (10.6–27.0)	1.26 (0.60–2.67)	0.544	1.37 (0.61–3.06)	0.445
High (>22.1)	132	5,349.3	10	10.5 (5.5–19.7)	0.73 (0.32–1.69)	0.465	0.71 (0.29–1.72)	0.450
Serum lycopene							*p* for trend	0.286
Low (<19.8)	129	4,827.0	15	17.5 (10.5–28.3)	1.00		1.00	
Medium (19.8–35.8)	131	4,954.6	11	10.0 (5.6–17.6)	0.71 (0.33–1.55)	0.395	0.61 (0.27–1.36)	0.223
High (>35.8)	131	5,065.5	12	13.1 (7.3–22.9)	0.76 (0.36–1.63)	0.48	0.73 (0.33–1.59)	0.428
Serum α-tocopherol							*p* for trend	0.788
Low (<753.0)	128	5,143.1	11	12.0 (6.6–21.2)	1.00		1.00	
Medium (753.0–983.9)	132	5,052.6	11	13.3 (7.4–23.3)	1.01 (0.44–2.33)	0.983	0.91 (0.39–2.10)	0.820
High (>983.9)	131	4,651.4	16	15.7 (9.3–25.8)	1.60 (0.74–3.45)	0.232	1.87 (0.84–4.19)	0.126
Retinol intake							*p* for trend	0.666
Low (<190.2)	130	4,778.5	14	14.7 (8.6–24.4)	1.00		1.00	
Medium (190.2–313.1)	130	4,985.2	15	16.7 (9.8–27.7)	1.02 (0.49–2.12)	0.948	1.08 (0.51–2.32)	0.834
High (>313.1)	131	5,083.4	9	9.5 (4.9–17.7)	0.60 (0.26–1.40)	0.239	0.62 (0.23–1.68)	0.346
Carotene intake							*p* for trend	0.331
Low (<3,281.4)	130	4,578.9	9	10.8 (5.2–21.6)	1.00		1.00	
Medium (3,281.4–5,042.8)	131	4,789.0	16	17.6 (11.4–26.7)	2.02 (0.91–4.46)	0.083	2.30 (0.97–5.42)	0.058
High (>5,042.8)	130	5,479.2	10	11.6 (6.2–21.0)	0.94 (0.38–2.33)	0.901	1.19 (0.41–3.44)	0.746
Vitamin A intake							*p* for trend	0.493
Low (<2,398.8)	130	4,510.5	11	12.2 (6.3–22.9)	1.00		1.00	
Medium (2,398.8–3,466.7)	131	4,921.0	16	15.1 (9.4–23.9)	1.33 (0.62–2.87)	0.463	1.32 (0.59–2.97)	0.500
High (>3,466.7)	130	5,415.6	11	12.6 (3.8–22.2)	0.84 (0.36–1.95)	0.689	0.92 (0.33–2.54)	0.873
Vitamin E intake							*p* for trend	0.834
Low (<6.7)	130	4,431.0	12	13.8 (7.5–24.7)	1.00		1.00	
Medium (6.7–8.7)	130	5,128.1	15	14.1 (8.6–22.6)	1.08 (0.51–2.31)	0.842	1.06 (0.44–2.56)	0.892
High (>8.7)	131	5,288.0	11	12.5 (6.8–22.1)	0.78 (0.34–1.77)	0.55	1.00 (0.30–3.38)	0.998

Cox's proportional hazard model showing the hazard ratio for progression over a cumulative 60-month period. The adjusted model was identical to the model used in Table 3. The units of micronutrients are expressed as μg/dL

effects were weaker or not found with a higher level of serum beta-carotene (HR 0.52, 95 % CI 0.24–1.13, $p = 0.098$). In contrast, a high carotene intake did not show an inverse relationship, but rather a non-significant increase in progression (HR 2.30, 95 % CI 0.97–5.42, $p = 0.058$). There was no significant association between other serum micronutrients and risk for CIN progression.

Discussion

The role of environmental factors, including micronutrients and tobacco smoking, in cervical carcinogenesis has been discussed. Smoking status in particular interfered with serum levels and intake of carotenoids as shown in Tables 1 and 2. In smokers, food intake is intrinsically lower than in non-smokers [22]. From the questionnaires, the intake per day of all micronutrients, except retinol and tocopherol, was lower in current smokers than in non-smokers, suggesting an unbalanced diet resulting from either smoking or other lifestyle behaviors (Table 1). Serum levels of alpha-carotene, beta-carotene and cryptoxanthin were inversely correlated with smoking status, but alpha-tocopherol was not correlated with smoking status after adjusting for age, BMI and frequency of alcohol intake (Table 2). These data were consistent with a previous report in which smoking was shown to affect serum beta-carotene levels but to have no effect on alpha-tocopherol levels [23]. Though alpha-tocopherol and beta-carotene are well known as antioxidants, the antioxidant effect of alpha-tocopherol is not due to a reaction with oxygen. In contrast, beta-carotene does react with oxygen. This suggests that there is a difference in the mechanisms of antioxidant reaction [24].

In regression subjects, we expected to find a protective effect from high serum levels or intake of carotenoids; however, neither of these had protective effects. We assume that smoking status modulates dietary intake or serum levels of micronutrients. Therefore, we investigated the association between dietary intake or serum levels of micronutrients and CIN regression, taking into account smoking status (Tables 3, 4, 5). In non-smoking regression subjects, regression was significantly related to the serum levels of zeaxanthin/lutein. This relationship was not found in current smokers. In a similar example, an isoflavone has a protective effect for lung cancer, but the effect is abolished by smoking [25]. It was reported that zeaxanthin/lutein may be a useful marker of intake of leafy vegetables, spinach, green peas, broccoli and seaweed [26]. Zeaxanthin/lutein is chemically more hydrophilic than other carotenoids such as alpha- and beta-carotene, lycopene and beta-cryptoxanthin. The mechanisms of a potential protection against carcinogenesis may include: induction of apoptosis, inhibition of angiogenesis, enhancement of gap junction intercellular communication, induction of cell differentiation, prevention of oxidative damage, and modulation of the immune system. Serum levels of lutein have been inversely associated with cytochrome CYP1A2 activity, a hepatic enzyme responsible for the metabolic activity of a number of putative human carcinogens [27]. High serum levels of alpha-tocopherol tend to have an inhibitory effect on regression in smokers (Table 4). There is a similar effect in that supplemental vitamin E, presumably causing a high concentration of alpha-tocopherol, is associated with an increased risk of lung cancer, which was confined to current smokers [28]. Alpha-tocopherol is considered to be an antioxidant, but it might act as a pro-oxidant [24].

Though a weak and non-significant protective effect of dietary intake or low serum concentration of beta-carotene has been observed previously [10, 15, 29, 30], we found that a medium serum level of beta-carotene showed a significant protective effect on CIN progression, whereas this protective effect at higher serum levels of beta-carotene was weaker or abolished (Table 6). These data appear to be consistent with in-vitro experiments reporting that very high concentrations of beta-carotene decreased antioxidant and/or induced pro-oxidant effects [31, 32]. Based on epidemiological studies that have shown an association between a low intake of carotenes and human cancers [33], an intervention study was conducted for the prevention of lung cancer [34]. However, it was paradoxically reported that high serum levels of beta-carotene induced by oral supplements promoted lung cancer in male heavy smokers aged 50–69 years. In CIN, oral beta-carotene supplementation did not enhance CIN regression in a randomized, double-blind phase III trial [35]. One explanation for these failures may be that oral supplements induced extremely high serum levels of beta-carotene. Taken together, these data suggest that medium serum levels of beta-carotene may interfere with CIN progression or cancer development.

There was a discrepancy between the results of dietary intake and serum levels of beta-carotene. Endogenous metabolic processes may influence the serum concentrations of micronutrients. In fact, inconsistent results of the serum levels and dietary intake of alpha-tocopherol in patients with prostate cancer, and contradictory results of retinol in patients with cervical cancer, have been reported previously [14, 36, 37]. Additionally, there is limited dietary intake information obtained from questionnaires because of inherent recall bias. We examined the residual confounding factors, including passive smoking, the number of sexual partners, and serum *Chlamydia* IgG antibody, in addition to the adjusted model. Despite confounding by other risk factors included for adjustments, the analyses did not change the conclusion.

To our knowledge, this is the first large-scale prospective cohort study for CIN outcome to report an association between serum levels of antioxidant micronutrients adjusted for potential confounders including CIN grade, HPV genotype, age, total energy intake and smoking. To make our comparisons, we investigated not only serum levels but also dietary intake of micronutrients, despite the fact that food-intake questionnaires contain limited information. It is known that the accuracy of recalling past dietary intake is influenced by current dietary habits [38]. There are inconsistent results between previous case–control and cohort studies. However, our discrepant results did not reach the conclusion that women with CIN received a benefit from consuming a beta-carotene-rich diet. However, not smoking and maintaining high serum levels of zeaxanthin/lutein, presumably by intake of leafy vegetables, spinach, green peas, broccoli, and seaweed, are advantageous for the prevention of cervical cancer.

This study has some potential limitations. We included only CIN patients with an available serum sample for measurement of serum nutrients [18]. The majority of CIN patients already had persistent HPV infection at enrollment in the present study. If these nutrients play an important role in preventing persistent HPV infection, we cannot determine that role in this cohort study. The food intake contains not only the micronutrients being investigated but also other nutrients and mixtures. The incident number of progression cases was small and it was difficult to analyze by smoking status. A large-scale cohort study with a longer period of observation is required to clarify the association between serum levels or dietary intake of micronutrients and the risk of developing cervical cancer.

Acknowledgments The authors thank: Dr. Tadahito Kanda (Center for Pathogen Genomics, National Institute of Infectious Disease, Tokyo, Japan) for his comments on the study design and the manuscript; the late Mr. Masafumi Tsuzuku (Department of Cytopathology, Cancer Institute Hospital, Japanese Foundation of Cancer Research, Japan) for his cytological review; many others who facilitated this study; and all of the women who participated in the study. This work was supported by a grant from the Ministry of Education, Culture, Sports, Science and Technology of Japan (Grant Number 12218102) and in part by a grant from the Smoking Research Foundation.

Conflict of interest The authors declare that they have no conflict of interest.

References

1. Syrjnen K, Hakama M, Saarikoski S et al (1990) Prevalence, incidence, and estimated life-time risk of cervical human papillomavirus infections in a nonselected Finnish female population. Sex Transm Dis 17:15–19
2. Schiffman M, Castle PE, Jeronimo J et al (2007) Human papillomavirus and cervical cancer. Lancet 370:890–907
3. Castellsague X, Bosch FX, Munoz N (2002) Environmental co-factors in HPV carcinogenesis. Virus Res 89:191–199
4. Jordan JA, Singer A (eds) (2006) The cervix, 2nd edn. Blackwell Publishing Ltd, Malden
5. Giuliano AR (2000) The role of nutrients in the prevention of cervical dysplasia and cancer. Nutrition 16:570–573
6. González CA, Travier N, Luján-Barroso L et al (2011) Dietary factors and in situ and invasive cervical cancer risk in the European prospective investigation into cancer and nutrition study. Int J Cancer 129:449–459
7. Ghosh C, Baker JA, Moysich KB et al (2008) Dietary intakes of selected nutrients and food groups and risk of cervical cancer. Nutr Cancer 60:331–341
8. Tomita LY, Longatto Filho A, Costa MC et al (2010) Diet and serum micronutrients in relation to cervical neoplasia and cancer among low-income Brazilian women. Int J Cancer 126:703–714
9. Cho H, Kim MK, Lee JK et al (2009) Relationship of serum antioxidant micronutrients and sociodemographic factors to cervical neoplasia: a case–control study. Clin Chem Lab Med 47:1005–1012
10. García-Closas R, Castellsagu X, Bosch X, González CA (2005) The role of diet and nutrition in cervical carcinogenesis: a review of recent evidence. Int J Cancer 117:629–637
11. Rock CL, Michael CW, Reynolds RK et al (2000) Prevention of cervix cancer. Crit Rev Oncol Hematol 33:169–185
12. Steinmetz KA, Potter JD (1996) Vegetables, fruit, and cancer prevention: a review. J Am Diet Assoc 96:1027–1039
13. Mascio P, Murphy M, Sies H (1991) Antioxidant defense systems: the role of carotenoids, tocopherols, and thiols. Am J Clin Nutr 53:194S–200S
14. Nagata C, Shimizu H, Higashiiwai H et al (1999) Serum retinol level and risk of subsequent cervical cancer in cases with cervical dysplasia. Cancer Invest 17:253–258
15. Sedjo RL, Papenfuss MR, Craft NE et al (2003) Effect of plasma micronutrients on clearance of oncogenic human papillomavirus (HPV) infection (United States). Cancer Causes Control 14:319–326
16. Nagata C, Shimizu H, Yoshikawa H et al (1999) Serum carotenoids and vitamins and risk of cervical dysplasia from a case–control study in Japan. Br J Cancer 81:1234–1237
17. Matsumoto K, Oki A, Furuta R et al (2010) Tobacco smoking and regression of low-grade cervical abnormalities. Cancer Sci 101:2065–2073
18. Matsumoto K, Oki A, Furuta R et al (2011) Predicting the progression of cervical precursor lesions by human papillomavirus genotyping: a prospective cohort study. Int J Cancer 128:2898–2910
19. Takatsuka N, Kurisu Y, Nagata C et al (1997) Validation of simplified diet history questionnaire. J Epidemiol 7:33–41
20. Yoshikawa H, Kawana T, Kitagawa K et al (1991) Detection and typing of multiple genital human papillomaviruses by DNA amplification with consensus primers. Jpn J Cancer Res 82:524–531
21. Miller KW, Yang CS (1985) An isocratic high-performance liquid chromatography method for the simultaneous analysis of plasma retinol, alpha-tocopherol, and various carotenoids. Anal Biochem 145:21–26
22. Tomita LY, Roteli-Martins CM, Villa LL et al (2011) Associations of dietary dark-green and deep-yellow vegetables and fruits with cervical intraepithelial neoplasia: modification by smoking. Br J Nutr 105:928–937
23. Palan PR, Mikhail MS, Basu J et al (1991) Plasma levels of antioxidant β-carotene and α-tocopherol in uterine cervix dysplasias and cancer. Nutr Cancer 15:13–20
24. Schneider C (2005) Chemistry and biology of vitamin E. Mol Nutr Food Res 49:7–30

25. Shimazu T, Inoue M, Sasazuki S et al (2010) Isoflavone intake and risk of lung cancer: a prospective cohort study in Japan. Am J Clin Nutr 91:722–728
26. Ito Y, Shimizu H, Yoshimura T et al (1999) Serum concentrations of carotenoids, alpha-tocopherol, fatty acids, and lipid peroxides among Japanese in Japan, and Japanese and Caucasians in the US. Int J Vitamin Nutr Res 69:385–395
27. Ribaya-Mercado JD, Blumberg JB (2004) Lutein and zeaxanthin and their potential roles in disease prevention. J Am Coll Nutr 23:567S–587S
28. Slatore CG, Littman AJ, Au DH et al (2008) Long-term use of supplemental multivitamins, vitamin C, vitamin E, and folate does not reduce the risk of lung cancer. Am J Respir Crit Care Med 177:524–530
29. Giuliano AR, Papenfuss M, Nour M et al (1997) Antioxidant nutrients: associations with persistent human papillomavirus infection. Cancer Epidemiol Biomarkers Prev 6:917–923
30. Giuliano AR, Siegel EM, Roe DJ et al (2003) Dietary intake and risk of persistent human papillomavirus (HPV) infection: the Ludwig–McGill HPV Natural History Study. J Infect Dis 188:1508–1516
31. El-Agamey A, Lowe GM, McGarvey DJ et al (2004) Carotenoid radical chemistry and antioxidant/pro-oxidant properties. Archiv Biochem Biophys 430:37–48
32. Burton GW, Ingold K (1984) Beta-carotene: an unusual type of lipid antioxidant. Science 224:569–573
33. Peto R, Doll R, Buckley JD et al (1981) Can dietary beta-carotene materially reduce human cancer rates? Nature 290:201–208
34. Alberts D, Barakat R (1994) The effect of vitamin E and beta carotene on the incidence of lung cancer and other cancers in male smokers. The Alpha-Tocopherol, Beta Carotene Cancer Prevention Study Group. N Engl J Med 330:1029–1035
35. Keefe KA, Schell MJ, Brewer C et al (2001) A randomized, double blind, Phase III trial using oral beta-carotene supplementation for women with high-grade cervical intraepithelial neoplasia. Cancer Epidemiol Biomarkers Prev 10:1029–1035
36. Weinstein SJ, Wright ME, Lawson KA et al (2007) Serum and dietary vitamin E in relation to prostate cancer risk. Cancer Epidemiol Biomarkers Prev 16:1253–1259
37. Kanetsky PA, Gammon MD, Mandelblatt J et al (1998) Dietary intake and blood levels of lycopene: association with cervical dysplasia among non-Hispanic, black women. Nutr Cancer 31:31–40
38. Myung SK, Ju W, Kim SC et al (2011) Vitamin or antioxidant intake (or serum level) and risk of cervical neoplasm: a meta-analysis. BJOG 118:1285–1291

Sequential effects of the proteasome inhibitor bortezomib and chemotherapeutic agents in uterine cervical cancer cell lines

YUICHIRO MIYAMOTO[1], SHUNSUKE NAKAGAWA[3], OSAMU WADA-HIRAIKE[1], TAKAYUKI SEIKI[1], MICHIHIRO TANIKAWA[1], HARUKO HIRAIKE[1], KENBUN SONE[1], KAZUNORI NAGASAKA[1], KATSUTOSHI ODA[1], KEI KAWANA[1], KEIICHI NAKAGAWA[2], TOMOYUKI FUJII[1], TETSU YANO[1], SHIRO KOZUMA[1] and YUJI TAKETANI[1]

Departments of [1]Obstetrics and Gynecology, and [2]Radiology, Graduate School of Medicine, The University of Tokyo, Tokyo 113-8655; [3]Department of Obstetrics and Gynecology, School of Medicine, Teikyo University, Tokyo 173-8605, Japan

Received August 8, 2012; Accepted September 10, 2012

DOI: 10.3892/or.2012.2072

Abstract. Although the prognosis of uterine cervical cancer has improved due to the advances of treatment modalities, survival of recurrent or metastatic cervical cancer remains poor. Cisplatin is an effective radiosensitizer, but its single agent activity in recurrent cervical cancer is disappointing. Inactivation of tumor suppressors through ubiquitin-mediated degradation by human papillomavirus is known to be a critical step in the carcinogenesis of uterine cervix. Bortezomib, a selective inhibitor of the proteasome, has been shown to inhibit the growth of several solid tumors. To determine the role of bortezomib in cervical cancer as a chemotherapeutic agent, we studied its biological properties. Bortezomib efficiently inhibited the proteasomal activities in cervical cancer cells, and an increased expression of tumor suppressors such as p53, hDlg and hScrib became evident. In addition, sequential or concomitant treatment of bortezomib and cisplatin stimulated the expression of p53, hScrib and p21 and the stimulation was markedly influenced by the order of drugs in HeLa cells. We further confirmed that the concomitant use of bortezomib and cisplatin has synergistic inhibitory effects on the growth of xenograft tumors derived from HeLa cells. Our data establish the possibility that the concomitant use of bortezomib and cisplatin could be an alternative choice in cases resistant to conventional chemotherapy, and sequential effects must be considered for advanced and therapy-resistant cervical cancer patients.

Correspondence to: Dr Shunsuke Nakagawa, Department of Obstetrics and Gynecology, School of Medicine, Teikyo University, 2-11-1 Kaga, Itabashi-ku, Tokyo 173-8605, Japan
E-mail: nakagawas-tky@umin.ac.jp

Key words: bortezomib, cell growth, cervical cancer, cisplatin, combination therapy, proteasome inhibitor

Introduction

Cancer of the uterine cervix is the second most common cause of gynecologic cancer mortality worldwide, and it is reported that cervical cancer affected 493,243 women worldwide in 2002 (1). It remains a health threat with estimated incidence and mortality rates of 12,710 and 4,290 in 2011, respectively, in the United States (2). Cervical cancer is now considered a preventable disease (3), but it is important to note that cervical cancer affects young women at a higher incidence. Treatment paradigms in the primary management of cervical cancer are well established. Early stage patients are treated surgically and women with locally advanced disease are managed with concomitant cisplatin chemoradiotherapy. However, the prognosis of patients with metastatic, recurrent, or persistent cervical cancer remains poor with a 1-year survival rate between 15-20% (4). In addition, chemotherapy has not led to major improvements in clinical outcome and is associated with high rates of severe toxicities. Advanced cervical cancer is associated with significant morbidities such as renal failure, complex fistulas and painful bone metastases. Therefore, improvement of systemic chemotherapy is crucial and new regimens should be further developed.

Persistent infection with an oncogenic-type human papillomavirus (HPV) is thought to be a prerequisite for the development of cervical cancer. The two HPV oncogenes, E6 and E7, are required for efficient immortalization of primary epithelial keratinocytes. The E6 proteins form a complex with p53 (5,6), and subsequent disruption of multiple functions of p53 is an important step in cervical carcinogenesis (7). E6 also affects the function of tumor suppressors involved in apoptosis, cell cycle regulation, and tissue polarity, including two human homologues of *Drosophila* neoplastic tumor suppressors, hDlg and hScrib (8,9).

Recent evidence indicates that rapidly proliferating cells, particularly cancer cells, have a greater requirement for proteasomal activity and a greater sensitivity to the proteasome inhibitor compared to normal cells (10). Bortezomib, a proteasome inhibitor, has been approved by the United

States Food and Drug Administration for the treatment of multiple myeloma, and bortezomib has shown *in vitro* and *in vivo* activity against solid tumors, including prostate, pancreatic and colon cancer (11). In gynecologic cancers, several investigators have reported implicative roles of bortezomib for the treatment of human cervical (12-16) and ovarian cancer (17).

In this study, we report that sequential or concomitant use of bortezomib with cisplatin markedly induces apoptosis and inhibition of growth in cultured cervical cancer cells and xenograft. Bortezomib may have pre-clinical activity in cisplatin-resistant tumors and may have synergic activity when combined with cisplatin in HeLa cells. These effects may have an important clinical implication to maximize the stabilization of tumor suppressors (18).

Materials and methods

Chemicals and antibodies. Bortezomib (VELCADE, formerly known as PS-341) was kindly provided by Millennium Pharmaceuticals (Cambridge, MA, USA). Cisplatin, carboplatin and paclitaxel were from Bristol-Myers Squibb (Princeton, NJ, USA). Bortezomib, cisplatin, carboplatin and paclitaxel were dissolved in dimethyl sulfoxide and the final concentration of dimethyl sulfoxide never exceeded 0.05%.

Anti-hScrib, anti-pRb (Ser 795), anti-p53 and anti-p21 were purchased from Santa Cruz Biotechnology (Santa Cruz, CA, USA). Rabbit polyclonal antibody was anti-Noxa (AnaSpec, Inc., San Jose, CA, USA). Mouse monoclonal antibody was anti-α-Tubulin (Calbiochem, EMD Biosciences, Inc., La Jolla, CA, USA). Alexa Fluor 488-conjugated donkey anti-mouse IgG (A-21202) and Alexa Fluor 555-conjugated goat anti-rabbit IgG (A-21428) were purchased from Invitrogen (Carlsbad, CA, USA).

Cell culture. HeLa (CCL-2) and CaSki (HB-8307) uterine cervical cancer cell lines were purchased from the American Type Culture Collection (Manassas, VA, USA) and grown in DMEM supplemented with 10% fetal bovine serum.

Sequential and simultaneous treatment regimens. To determine the effect of sequence difference on cellular response, cells were treated with bortezomib (100 nM), carboplatin (250 μM), paclitaxel (10 μM) and cisplatin (500 μM). HeLa and CaSki cells were seeded and allowed to adhere for 24 h. For the sequential treatment, after 12 h of initial treatment, the medium was changed to fresh medium containing the other treatment. For the simultaneous treatment, after an initial 12 h in medium, cells were treated with fresh medium containing the same drugs. The control cell medium was changed at similar time points. After the second 12-h treatment, the cells were harvested for flow cytometric analysis or western blotting. Therefore, all groups received the same duration of exposure to each agent and the assays were performed at the same point following the final treatment.

Cell viability test. Viability of HeLa and CaSki cells was examined using the CellTiter 96 Aqueous One Solution Cell Proliferation Assay kit (Promega Corp., Madison, WI, USA), as previously described (19).

Pulse chase analysis of p53 and hScrib. The culture medium of HeLa cells was replaced with Met/Cys-free DMEM for 2 h and pulsed with 20 μCi/ml of EasyTag™ EXPRESS^{35}S (Perkin-Elmer Life Sciences, Boston, MA, USA) for 1.5 h. The ^{35}S-labeled protein was chased with or without bortezomib (100 nM). Cells were harvested at the indicated time point, lysed and electrophoresed.

Western blotting. Cultured cells and mouse xenograft tissues were harvested and soluble protein was extracted. The procedure of western blotting and subsequent immunoblot was performed as previously described (20).

Flow cytometric analysis. To determine the apoptosis rate, cells were grown in DMEM and treated with chemotherapeutic drugs. Bortezomib, cisplatin, carboplatin and paclitaxel treatments in 12-h increments over a 24-h period were as described. Following treatment, cells were harvested and stained with Annexin V-FITC and propidium iodide (PI) according to the manufacturer's protocol (BD Biosciences, Bedford, MA, USA). The percentage of specific apoptosis was analyzed on FACSCalibur and calculated by CELLQuest Pro software (BD Biosciences).

Quantification of the synergism of bortezomib with cisplatin in the manner of sequential or simultaneous administration (Chou-Talalay assay). For the Chou-Talalay assay, experiments were carried out as previously described (21). Dose-response curves and 50% effective dose values (ED_{50}) were obtained, and fixed ratios of drugs and mutually exclusive equations used to determine combination indices (CI) (22). The potency of the combination was calculated with the CalcuSyn software (Biosoft, Ferguson, MO, USA). CI<1, CI=1, and CI>1 indicate synergistic, additive and antagonistic interactions, respectively.

Tumor growth suppression in vivo. Athymic C.B-17/Icr-scid Jcl mice 5-7 weeks of age (CLEA Japan, Inc., Tokyo, Japan) were maintained in an SPF facility according to the institutional guidelines, and experiments were conducted under an approved animal protocol of The University of Tokyo. Subcutaneous xenograft tumors were established by the injection of cell suspension of $1x10^7$ HeLa and CaSki cells. After the appropriate tumors were formed, the mice were sacrificed. The tumors were removed, cut into 3-mm sections and transplanted subcutaneously into other mice. Mice were randomly assigned to one of the four treatment regimens: saline (control), cisplatin [intraperitoneal (i.p.) injection of cisplatin at a dose of 6 mg/kg in a volume of 0.5 ml (23)], bortezomib [i.p. injection of bortezomib at a dose of 1 mg/kg in a volume of 0.5 ml (24)], and bortezomib followed by cisplatin 8 h later in a combined volume of 0.5 ml. Each treatment group consisted of 6 mice. Tumors were measured and the volume of these tumors was calculated using the formula; Volume (mm^3) = [(major axis) x (minor axis)^2]/2. After 4 weeks of treatment, the mice were sacrificed and subjected to the analysis.

Immunofluorescence. The mouse xenograft tumors were frozen in OCT compounds (Sakura Finetek Japan Co., Ltd., Tokyo, Japan). The embedded tissues were cut (6 μm) and cryostat sections were recovered and fixed with PBS containing

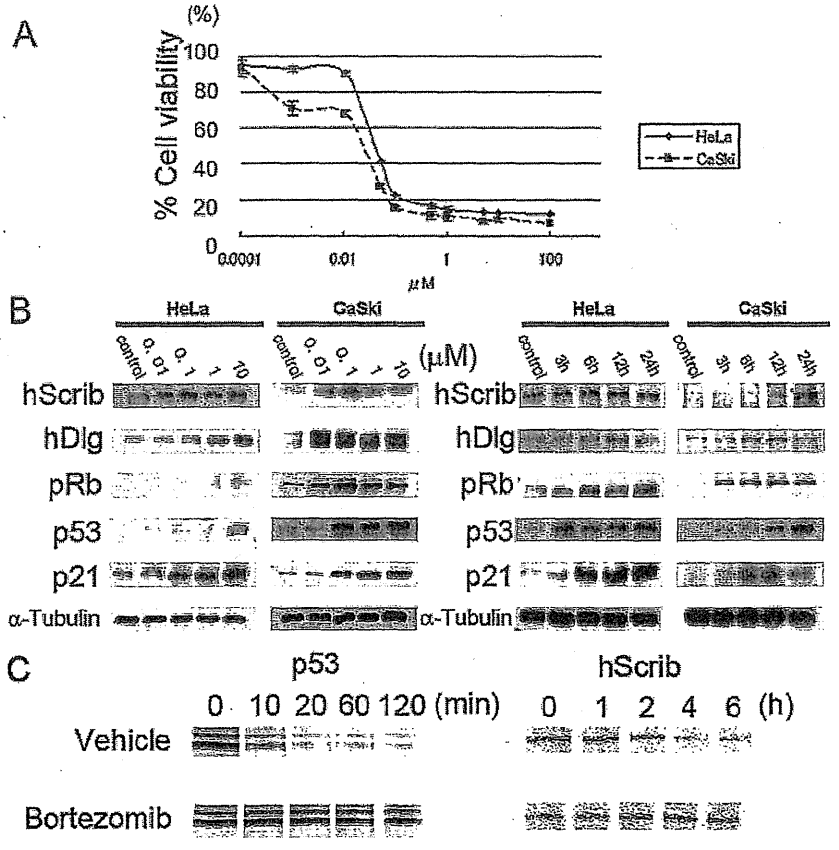

Figure 1. Biological effects of bortezomib on human cervical cancer cell lines and stabilization of tumor suppressors. (A) HeLa and CaSki cells were exposed to bortezomib for 48 h and cell viability was determined by MTS assay. Each point represents the means ± SD of 3 independent experiments. (B) The effect of bortezomib on the expression of tumor suppressor proteins. (1) HeLa and CaSki cells were exposed to various concentrations of bortezomib for 12 h (left panel). (2) Cells treated by 100 nM of bortezomib were harvested at the indicated time points (right panel). The expression levels of hScrib, hDlg, pRb, p53 and p21 were analyzed by western blotting. (C) Pulse chase analysis of p53 and hScrib. p53 and hScrib proteins were ^{35}S-labeled in HeLa cells and the amount of labeled proteins were chased in the presence and absence of bortezomib. In the presence of bortezomib, the expression of p53 and hScrib remained unaffected during the observed time.

4% paraformaldehyde. After blocking, the cells were sequentially incubated with anti-p53 or anti-hScrib antibodies and appropriate secondary antibodies. The slides were briefly counterstained and analyzed under the fluorescence microscope (Olympus BX50; Olympus, Tokyo, Japan). Apoptotic cells were detected by DeadEnd™ Fluorometric TUNEL System (Promega Corp.) in the mouse xenograft tumors.

Statistical analysis. Data represent the means ± SD or SEM from at least 3 independent experiments. Statistical analyses were performed by one-way ANOVA with post-hoc test for multiple comparisons by using StatView software (SAS Institute Inc., Cary, NC, USA). A P-value <0.05 was considered to indicate statistically significant differences.

Results

Effect of bortezomib on cellular viability and stabilization of tumor suppressor proteins targeted for degradation by HPV E6 and E7 in human cervical cancer cell lines. We used MTS assay to determine the effect of bortezomib on cell viability in HeLa and CaSki cells (Fig. 1A). The approximately estimated IC_{50} of bortezomib in HeLa and CaSki cells was 100 nM. The expression of p53 increased by the exposure to bortezomib in a dose-dependent manner (Fig. 1B left panel) and in a time-dependent manner (Fig. 1B right panel). As a result, the expression of p21 also increased. Elevated expression of PDZ domain-containing scaffolding proteins (hScrib and hDlg) was shown by the exposure to bortezomib (Fig. 1B). The expression of pRb decreases by the proteasome system during cervical carcinogenesis (25), and the expression of pRb was remarkably stimulated by the addition of bortezomib, particularly in CaSki cells (Fig. 1B). These data were translated as the antitumorigenic properties of bortezomib and we further confirmed whether p53 and hScrib are stabilized in the presence of bortemozib by the pulse-chase analysis. As expected, p53 and hScrib expression remained unaffected in the presence of bortezomib in HeLa cells (Fig. 1C).

Effect of bortezomib and chemotherapeutic agents on cervical cancer cells. The effect of bortezomib and chemotherapeutic drugs on the induction of apoptosis was analyzed by the flow cytometric analysis (Fig. 2A). As a single agent, bortezomib (lane 2) possessed a significant ability to induce apoptosis compared to cisplatin, carboplatin, and paclitaxel (lanes 3, 4 and 5, respectively), and the rate of apoptosis was superior in CaSki cells. The sequential and simultaneous combination of bortezomib with cisplatin was identified to be the most

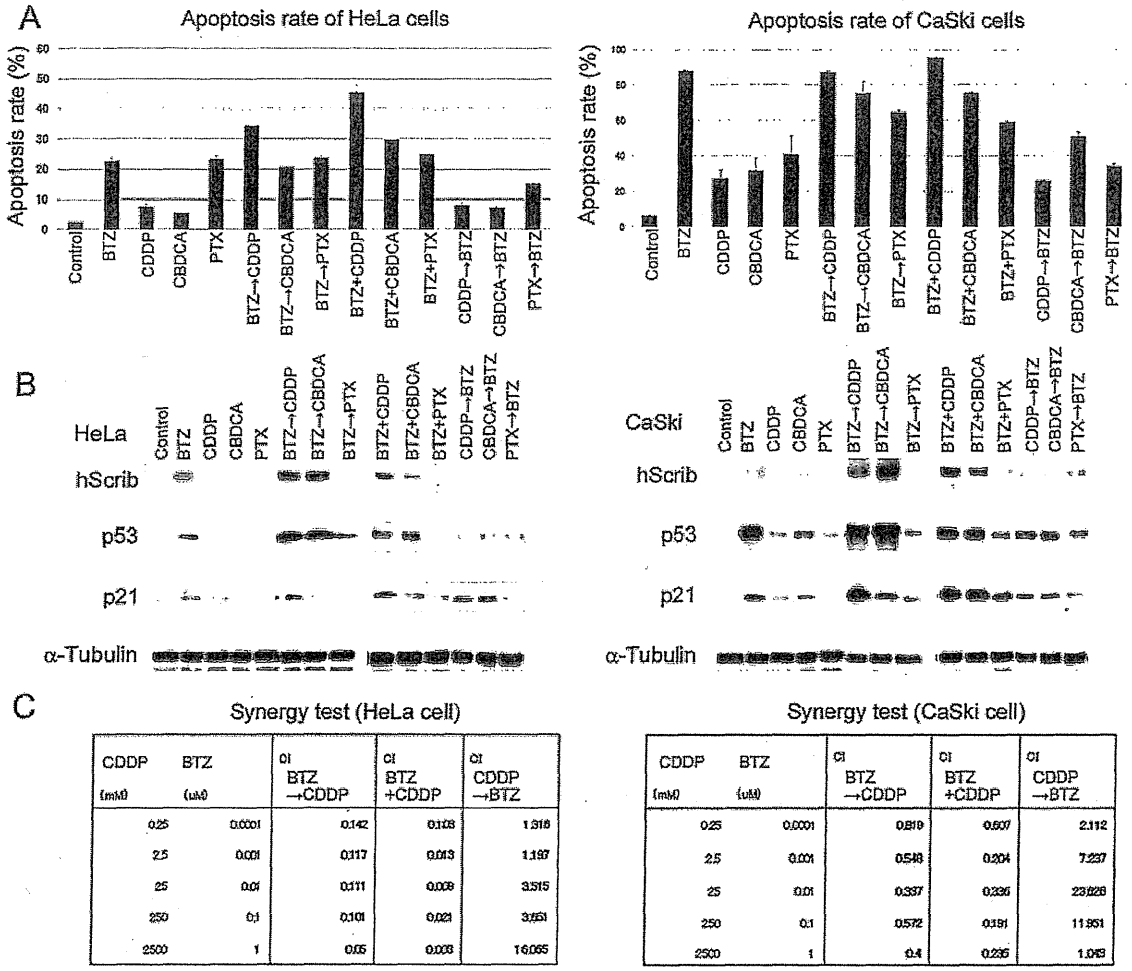

CDDP (mM)	BTZ (uM)	CI BTZ →CDDP	CI BTZ +CDDP	CI CDDP →BTZ
0.25	0.0001	0.142	0.108	1.318
2.5	0.001	0.117	0.013	1.197
25	0.01	0.111	0.009	3.515
250	0.1	0.101	0.021	3.651
2500	1	0.05	0.008	16.065

CDDP (mM)	BTZ (uM)	CI BTZ →CDDP	CI BTZ +CDDP	CI CDDP →BTZ
0.25	0.0001	0.819	0.607	2.112
2.5	0.001	0.548	0.204	7.237
25	0.01	0.337	0.336	23.828
250	0.1	0.572	0.191	11.951
2500	1	0.4	0.235	1.049

Figure 2. An analysis of bortezomib and chemotherapeutic drugs in cervical cancer cells. (A) The rate of apoptosis using bortezomib and chemotherapeutic drugs was measured by flow cytometric analysis. Single, sequential, or simultaneous treatment regimens using bortezomib (100 nM), cisplatin (500 μM), carboplatin (250 μM) or paclitaxel (10 μM) were applied for HeLa and CaSki cells. Bortezomib followed by cisplatin and concomitant bortezomib with cisplatin regimens induced higher apoptosis rates compared with other regimens. Bars represent the means ± SD of 3 independent experiments. (B) Bortezomib stabilized the expression of hScrib and p53 in cervical cancer cell lines in combination with platinum agents. By contrast, cisplatin followed by bortezomib failed to stimulate the expression of hScrib, p53 and p21. (C) Quantification of the potency of the combination treatment. The Chou-Talalay method was utilized. Bortezomib followed by cisplatin and concomitant bortezomib with cisplatin regimens exhibited synergistic effects in all the doses tested. A potent synergistic effect was displayed with CI<0.1. By contrast, a low synergistic or antagonistic effect was shown in the treatment using cisplatin followed by bortezomib with CI>1. BTZ, bortezomib; CDDP, cisplatin; CBDCA, carboplatin; PTX, paclitaxel.

significant treatment regimens in inducing cellular apoptosis (Fig. 2A, lanes 6 and 9) in HeLa cells.

We further investigated the expression of hScrib, p53 and p21, whether the apoptotic effects are indeed associated with protein expressions. Cells were exposed to various concentrations of bortezomib and/or chemotherapeutic drugs (Fig. 2B). The elevated expression of p53 was observed in HeLa cells treated with bortezomib followed by cisplatin or carboplatin (lanes 6 and 7), and in CaSki cells treated with bortezomib alone (lane 2), bortezomib followed by cisplatin or carboplatin (lanes 6 and 7). The expression of hScrib exhibited a similar tendency to that of p53. In terms of the stabilization of p53 and hScrib, paclitaxel turned out to be an unsatisfactory agent (lanes 5, 8, 11 and 14). Markedly, bortezomib and subsequent cisplatin treatment was the most efficient regimen to induce the expression of p21, particularly in CaSki cells (lane 6). Cisplatin followed by bortezomib treatment had an insignificant effect on the expression of p53 and hScrib (lane 12). The apparent recovery of pRb was also observed in HeLa cells treated by the exposure to bortezomib followed by cisplatin (data not shown).

The synergistic effects of bortezomib and cisplatin were analyzed using the Chou-Talalay assay. Bortezomib followed by cisplatin and simultaneous bortezomib with cisplatin regimens were synergistic, with CI<1. This synergy was evidently affected by the order of addition as cisplatin followed by bortezomib showed antagonistic interactions, with CI>1. Therefore, the synergistic effects in HeLa cells was more pronounced compared to that in CaSki cells and we determined to pursue the sequential effect of bortezomib and cisplatin.

In vivo suppression of cervical cancer growth by bortezomib in a mouse xenograft. We analyzed whether bortezomib is able to inhibit tumor growth using a xenograft mouse model of cervical cancer cells. Bortezomib was administered twice a

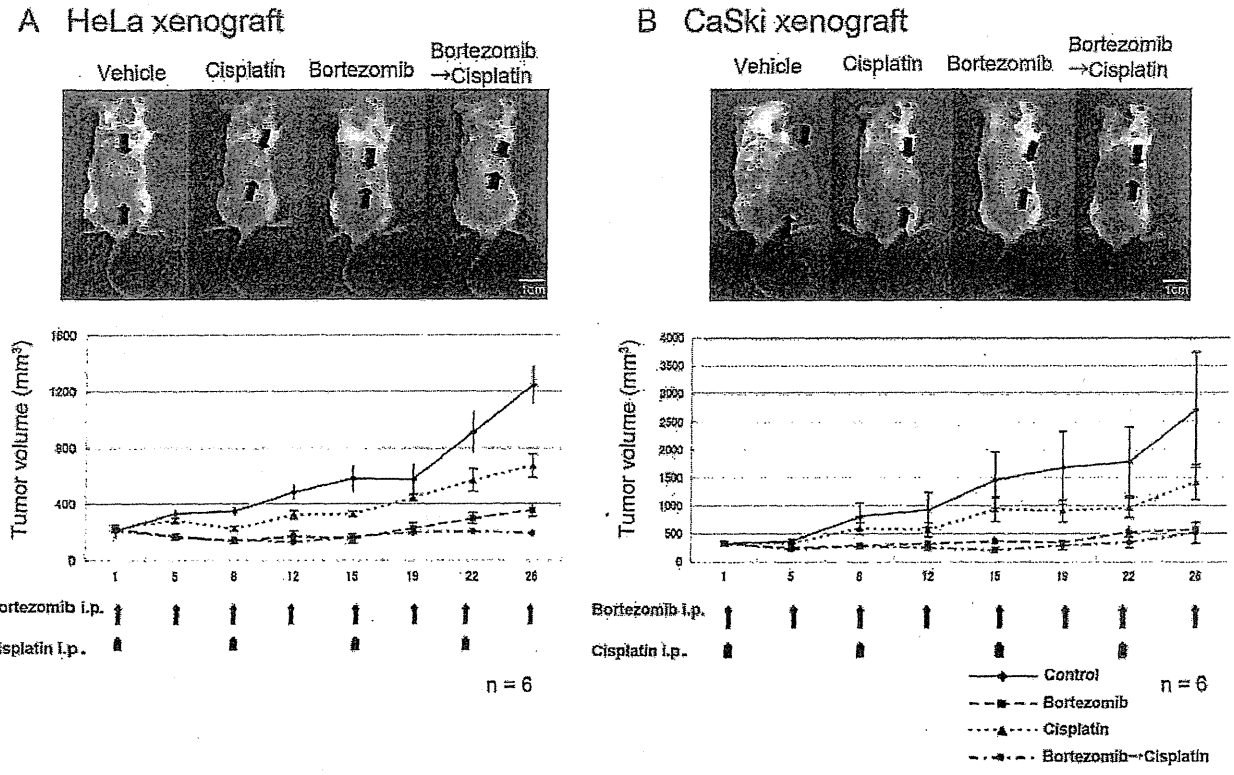

Figure 3. Bortezomib and bortezomib with cisplatin efficiently inhibited the growth of cervical cancer xenografts in athymic mice. (A) Representative images of xenograft mice are shown. Bars indicate 1 cm. (B) HeLa and CaSki cells were transplanted into 6 to 7-week-old athymic mice. When xenograft tumors were visualized, 4 treatment regimens were commenced. Treatment schedules are indicated by thin arrows (bortezomib) and thick arrows (cisplatin). The dose of bortezomib was 1 mg/kg, and the dose of cisplatin was 6 mg/kg, according to the recommendation of the suppliers. Each treatment group consisted of 6 mice. Tumor volumes were calculated as described in Materials and methods. Bars indicate the means ± SEM.

week, and cisplatin once a week according to the instructions of the suppliers. As shown in Fig. 3, the tumor volume of the HeLa and CaSki xenograft was significantly reduced by the injection of bortezomib when compared with the control. The reduction rate of the tumor growth in the bortezomib group was greater than that of cisplatin alone and we revealed that bortezomib with cisplatin was the most efficient treatment regimen in the HeLa xenograft. The CaSki xenograft exhibited a pronounced sensitivity to bortezomib alone and the effect of concomitant use was not observed as expected from the *in vitro* study (Fig. 2, right panel).

Based on the data in Fig. 2, the expression levels of p53, Noxa, and p21 in cervical cancer xenografts were analyzed by western blot analysis. It became evident that p53 and its downstream genes are upregulated in xenografts treated by bortezomib (Fig. 4A and B). Our immunofluorescence study also revealed that the expression of hScrib was recovered at the cellular membrane in mice treated with bortezomib alone or in combination with cisplatin (Fig. 4C and D). The expression of p53 in the nuclei of xenograft cells also increased as a result of treatment of bortezomib (Fig. 4C and D). HeLa and CaSki xenografts were subjected to the detection of apoptosis using TUNEL assay and TUNEL positive cells were observed predominantly in xenograft tumors treated by bortezomib (Fig. 4C and D). These data suggest the possibility that bortezomib inhibits tumor growth *in vivo* through the induction of apoptosis driven by p53 and downstream genes of p53, particularly in HeLa cells.

Discussion

Bortezomib has been shown to be an extremely potent, reversible and selective proteasome inhibitor (26). Several investigators have demonstrated the ability of bortezomib to sensitize a variety of cancer cells to the apoptotic effects of diverse chemotherapeutic agents (12-15,17,27-29). We confirmed that bortezomib was able to induce apoptosis in HPV-positive cervical cancer cell lines. Cisplatin, a critical component of therapeutic regimens in a broad range of malignancies, has been shown to induce apoptosis in various types of cancer cells. For the treatment of advanced or recurrent cervical cancer, cisplatin administered every 3 weeks seems to be a reasonable option, inducing response rates ranging from 20 to 30% and an overall survival of 7 months (30), but prolonged cisplatin treatment appears to have considerable side-effects. We aimed to explore the possibility that concomitant use of bortezomib and chemotherapeutic drugs has additive effects to suppress ubiquitin-mediated degradation of tumor suppressors targeted by E6 in HPV-positive cervical cancer cells both *in vitro* and *in vivo*. As expected, bortezomib alone increased the expression of tumor suppressors such as p53 and hScrib in a dose- and time-dependent manner. We also observed the elevated expression of p21 by the treatment of bortezomib since p21 is a representative downstream gene of p53. We noted that the rate of apoptosis in cells treated with bortezomib preceded by cisplatin was extremely lower than that in cells treated with cisplatin preceded by bortezomib in HeLa cells. The sequential

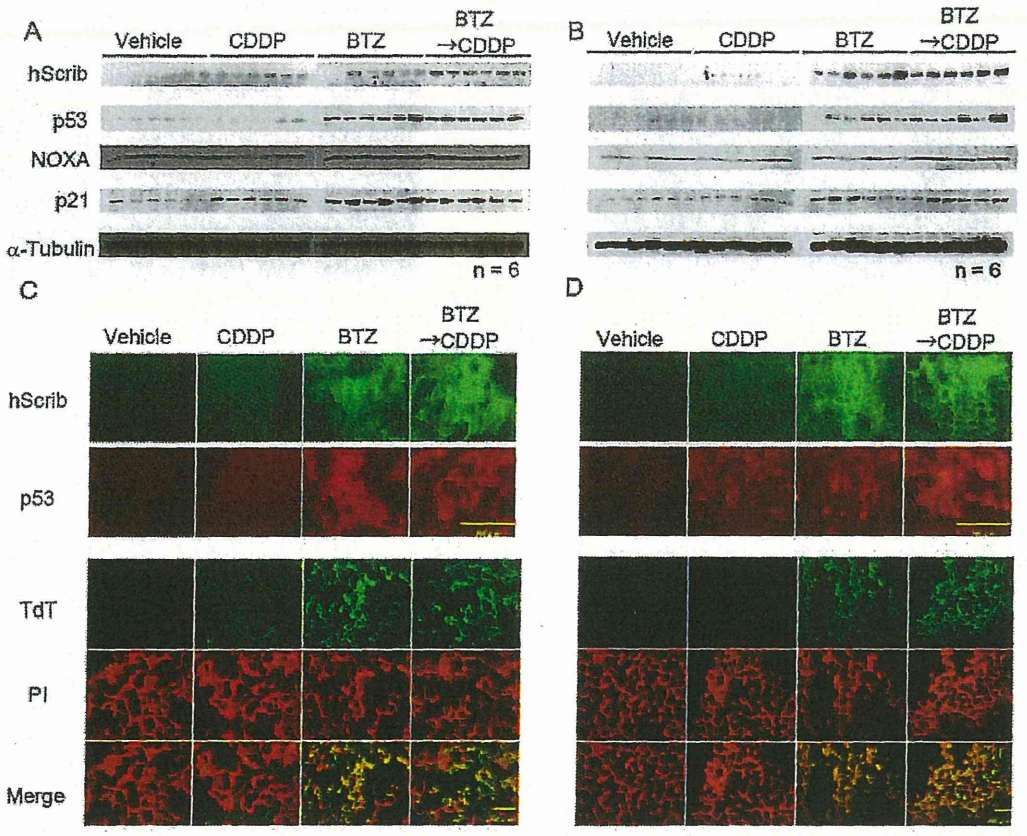

Figure 4. The growth inhibitory effect of bortezomib and cisplatin is evidenced by elevated expression of p53 and hScrib in xenografts of athymic mice. (A and B) Whole cell extracts were obtained from xenograft tumors and the expression levels of hScrib, p53, Noxa and p21 were analyzed by western blotting. (A) HeLa cell xenograft; (B) CaSki cell xenograft. (C and D) The expression levels of hScrib and p53 were visualized by immunofluorescence (upper panel). TUNEL assay revealed that bortezomib and concomitant use of bortezomib and cisplatin induced significant apoptosis in xenograft tumors (lower panel). (C) HeLa cell xenograft; (D) CaSki cell xenograft. Bars indicate 200 μm.

effect (bortezomib followed by cisplatin) on the induction of apoptosis was prominent compared with other combinations. However, this sequential effect was less pronounced in CaSki cells both *in vitro* and *in vivo*, and was similar to a previous report that bortezomib did not induce a sensitization to cisplatin treatment in SiHa cells (16). We must take into account the fact that bortezomib alone was able to induce significant apoptosis in CaSki cells (Fig. 2A, right panel), and this result is in concordance with the result of the Chou-Talalay assay that synergistic effects in HeLa cells were more pronounced compared to those in CaSki cells (Fig. 2C). The optimal sequence of chemotherapies with disparate mechanisms of action has been investigated intensively. Although the mechanisms of the sequence-specific interactions with chemotherapy remain unclear, one possible explanation could be the effect on the apoptotic mechanism by bortezomib. Cisplatin was shown to have a defect in mitochondria-dependent caspase-9 activation in non-small cell lung cancer H460 cells (29). Contrary to this, bortezomib efficiently induced caspase-9 activation and apoptosis by promoting a pro-apoptotic shift in the levels of proteins involved in mitochondrial outer-membrane permeabilization (29). Another mechanism might be its distribution to cell cycle arrest. Bortezomib causes G2/M arrest (31) and cisplatin causes long-lasting blocks at the G1/S boundary with increasing cytotoxicity (32). Theoretically, when bortezomib is administered first, the increased p53 may serve to enhance G1/S checkpoint function. Then G1/S arrest by cisplatin may efficiently enhance apoptotic cell death.

We further examined whether concomitant use of bortezomib and cisplatin can induce apoptosis *in vivo*. Although the regimen was not completely identical to that of the *in vitro* experiment, the concomitant use of bortezomib and cisplatin abrogated the tumor growth of xenografts. In bortezomib-treated tumors, p53 is apparently stabilized in the nuclei of tumor cells, and, subsequently, p21 and Noxa are elevated due to the increased expression of p53. TUNEL assay showed enhanced apoptosis in xenografts treated by bortezomib alone or bortezomib with cisplatin, but concomitant treatment showed significant enhancement of apoptosis. Several investigators have reported the sequence-dependent effects of bortezomib are limited (28,33). The optimal apoptotic effect occurs with the sequence gemcitabine followed by bortezomib in pancreatic cancer cells (33) and in lung cancer cells (28). Therefore, the effect of bortezomib may be sensitization of cancer cells to the apoptotic effect and may be modulating the cellular response to the chemotherapeutics. As a result, bortezomib may enhance cell death in combination with cisplatin. Our data provide new evidence that the schedule of combination treatment must be considered for the treatment of cervical cancer, and gynecologists should consider pre-clinical data in

the design of clinical trials. While it is important to confirm sequential effects in each cancer type studied, it appears that chemotherapy given prior to bortezomib may yield inferior results.

In conclusion, a proteasome inhibitor, bortezomib, induces apoptosis in HPV-positive cervical cancer cells depending on the stabilization of tumor suppressors, particularly p53. When bortezomib is combined with cisplatin, a higher effect of apoptosis induction might be expected since bortezomib plus cisplatin almost completely abolished growth of cervical cancer xenografts with the recovery of p53 and hScrib expression. Our data suggest the possibility that bortezomib plus cisplatin is a promising regimen for the treatment of advanced and/or chemotherapy or radiation therapy-resistant cervical cancer cases.

Acknowledgements

This study was supported by the Mitsui Life Social Welfare Foundation and the grant-in-aid for Scientific Research from the Ministry of Education, Science and Culture, Japan.

References

1. Parkin DM, Bray F, Ferlay J and Pisani P: Global cancer statistics, 2002. CA Cancer J Clin 55: 74-108, 2005.
2. American Cancer Society: Cancer Facts and Figures 2011. http://www.cancer.org/Cancer/CervicalCancer. 2011.
3. Carter JR, Ding Z and Rose BR: HPV infection and cervical disease: a review. Aust N Z J Obstet Gynaecol 51: 103-108, 2011.
4. Berek JS and Hacker NF (eds): Practical Gynaecologic Oncology. 4th edition. Lippincott Williams & Wilkins, Philadelphia, PA, 2005.
5. Nakagawa S, Watanabe S, Yoshikawa H, Taketani Y, Yoshiike K and Kanda T: Mutational analysis of human papillomavirus type 16 E6 protein: transforming function for human cells and degradation of p53 in vitro. Virology 212: 535-542, 1995.
6. Crook T, Tidy JA and Vousden KH: Degradation of p53 can be targeted by HPV E6 sequences distinct from those required for p53 binding and trans-activation. Cell 67: 547-556, 1991.
7. Huibregtse JM and Beaudenon SL: Mechanism of HPV E6 proteins in cellular transformation. Semin Cancer Biol 7: 317-326, 1996.
8. Massimi P, Gammoh N, Thomas M and Banks L: HPV E6 specifically targets different cellular pools of its PDZ domain-containing tumour suppressor substrates for proteasome-mediated degradation. Oncogene 23: 8033-8039, 2004.
9. Nakagawa S and Huibregtse JM: Human scribble (Vartul) is targeted for ubiquitin-mediated degradation by the high-risk papillomavirus E6 proteins and the E6AP ubiquitin-protein ligase. Mol Cell Biol 20: 8244-8253, 2000.
10. Mani A and Gelmann EP: The ubiquitin-proteasome pathway and its role in cancer. J Clin Oncol 23: 4776-4789, 2005.
11. Adams J and Kauffman M: Development of the proteasome inhibitor Velcade (Bortezomib). Cancer Invest 22: 304-311, 2004.
12. Birle DC and Hedley DW: Suppression of the hypoxia-inducible factor-1 response in cervical carcinoma xenografts by proteasome inhibitors. Cancer Res 67: 1735-1743, 2007.
13. Kamer S, Ren Q and Dicker AP: Differential radiation sensitization of human cervical cancer cell lines by the proteasome inhibitor velcade (bortezomib, PS-341). Arch Gynecol Obstet 279: 41-46, 2009.
14. Lin Z, Bazzaro M, Wang MC, Chan KC, Peng S and Roden RB: Combination of proteasome and HDAC inhibitors for uterine cervical cancer treatment. Clin Cancer Res 15: 570-577, 2009.
15. Jiang Y, Wang Y, Su Z, *et al*: Synergistic induction of apoptosis in HeLa cells by the proteasome inhibitor bortezomib and histone deacetylase inhibitor SAHA. Mol Med Rep 3: 613-619, 2010.
16. Bruning A, Vogel M, Mylonas I, Friese K and Burges A: Bortezomib targets the caspase-like proteasome activity in cervical cancer cells, triggering apoptosis that can be enhanced by nelfinavir. Curr Cancer Drug Targets 11: 799-809, 2011.
17. Frankel A, Man S, Elliott P, Adams J and Kerbel RS: Lack of multicellular drug resistance observed in human ovarian and prostate carcinoma treated with the proteasome inhibitor PS-341. Clin Cancer Res 6: 3719-3728, 2000.
18. Nagasaka K, Nakagawa S, Yano T, *et al*: Human homolog of *Drosophila* tumor suppressor Scribble negatively regulates cell-cycle progression from G1 to S phase by localizing at the basolateral membrane in epithelial cells. Cancer Sci 97: 1217-1225, 2006.
19. Morita Y, Wada-Hiraike O, Yano T, *et al*: Resveratrol promotes expression of SIRT1 and StAR in rat ovarian granulosa cells: an implicative role of SIRT1 in the ovary. Reprod Biol Endocrinol 10: 14, 2012.
20. Wada-Hiraike O, Yano T, Nei T, *et al*: The DNA mismatch repair gene hMSH2 is a potent coactivator of oestrogen receptor alpha. Br J Cancer 92: 2286-2291, 2005.
21. Chou TC: Drug combination studies and their synergy quantification using the Chou-Talalay method. Cancer Res 70: 440-446, 2010.
22. Kanai R, Wakimoto H, Martuza RL and Rabkin SD: A novel oncolytic herpes simplex virus that synergizes with phosphoinositide 3-kinase/Akt pathway inhibitors to target glioblastoma stem cells. Clin Cancer Res 17: 3686-3696, 2011.
23. Fraval HN and Roberts JJ: G1 phase Chinese hamster V79-379A cells are inherently more sensitive to platinum bound to their DNA than mid S phase or asynchronously treated cells. Biochem Pharmacol 28: 1575-1580, 1979.
24. Nawrocki ST, Bruns CJ, Harbison MT, *et al*: Effects of the proteasome inhibitor PS-341 on apoptosis and angiogenesis in orthotopic human pancreatic tumor xenografts. Mol Cancer Ther 1: 1243-1253, 2002.
25. Munger K and Howley PM: Human papillomavirus immortalization and transformation functions. Virus Res 89: 213-228, 2002.
26. Adams J: The proteasome: structure, function, and role in the cell. Cancer Treat Rev 29 (Suppl 1): 3-9, 2003.
27. Ling YH, Liebes L, Jiang JD, *et al*: Mechanisms of proteasome inhibitor PS-341-induced G(2)-M-phase arrest and apoptosis in human non-small cell lung cancer cell lines. Clin Cancer Res 9: 1145-1154, 2003.
28. Mortenson MM, Schlieman MG, Virudachalam S and Bold RJ: Effects of the proteasome inhibitor bortezomib alone and in combination with chemotherapy in the A549 non-small-cell lung cancer cell line. Cancer Chemother Pharmacol 54: 343-353, 2004.
29. Voortman J, Checinska A, Giaccone G, Rodriguez JA and Kruyt FA: Bortezomib, but not cisplatin, induces mitochondria-dependent apoptosis accompanied by up-regulation of noxa in the non-small cell lung cancer cell line NCI-H460. Mol Cancer Ther 6: 1046-1053, 2007.
30. Tewari KS and Monk BJ: Gynecologic oncology group trials of chemotherapy for metastatic and recurrent cervical cancer. Curr Oncol Rep 7: 419-434, 2005.
31. Gregory MA and Hann SR: c-Myc proteolysis by the ubiquitin-proteasome pathway: stabilization of c-Myc in Burkitt's lymphoma cells. Mol Cell Biol 20: 2423-2435, 2000.
32. Jackel M and Kopf-Maier P: Influence of cisplatin on cell-cycle progression in xenografted human head and neck carcinomas. Cancer Chemother Pharmacol 27: 464-471, 1991.
33. Fahy BN, Schlieman MG, Virudachalam S and Bold RJ: Schedule-dependent molecular effects of the proteasome inhibitor bortezomib and gemcitabine in pancreatic cancer. J Surg Res 113: 88-95, 2003.

ORIGINAL ARTICLE

The Prevalence of Cervical Regulatory T Cells in HPV-Related Cervical Intraepithelial Neoplasia (CIN) Correlates Inversely with Spontaneous Regression of CIN

Satoko Kojima[1], Kei Kawana[1], Kensuke Tomio[1], Aki Yamashita[1], Ayumi Taguchi[1], Shiho Miura[1], Katsuyuki Adachi[1], Takeshi Nagamatsu[1], Kazunori Nagasaka[1], Yoko Matsumoto[1], Takahide Arimoto[1], Katsutoshi Oda[1], Osamu Wada-Hiraike[1], Tetsu Yano[1], Yuji Taketani[1], Tomoyuki Fujii[1], Danny J. Schust[2], Shiro Kozuma[1]

[1]Department of Obstetrics and Gynecology, Faculty of Medicine, University of Tokyo, Bunkyo-ku, Tokyo, Japan;
[2]Division of Reproductive Endocrinology and Fertility, Department of Obstetrics, Gynecology and Women's Health, University of Missouri School of Medicine, Columbia, MO, USA

Keywords
CD4+CD25+Foxp3+ regulatory T cells, cervical intraepithelial neoplasia, cervical lymphocytes, programmed cell death-1

Correspondence
Kei Kawana, Department of Obstetrics and Gynecology, Faculty of Medicine, University of Tokyo, 7-3-1 Hongo, Bunkyo-ku, Tokyo 113-8655, Japan.
E-mail: kkawana-tky@umin.ac.jp

Submission June 24, 2012;
accepted September 13, 2012.

Citation
Kojima S, Kawana K, Tomio K, Yamashita A, Taguchi A, Miura S, Adachi K, Nagamatsu T, Nagasaka K, Matsumoto Y, Arimoto T, Oda K, Wada-Hiraike O, Yano T, Taketani Y, Fujii T, Schust DJ, Kozuma S. The prevalence of cervical regulatory T cells in HPV-related cervical intraepithelial neoplasia (CIN) correlates inversely with spontaneous regression of CIN. *Am J Reprod Immunol* 2013; 69: 134–141

doi:10.1111/aji.12030

Problem
Local adaptive cervical regulatory T cells (Tregs) are the most likely direct suppressors of the immune eradication of cervical intraepithelial lesion (CIN). PD-1 expression on T cells induces Tregs. No studies have quantitatively analyzed the Tregs and PD-1+ cells residing in CIN lesions.

Method of study
Cervical lymphocytes were collected using cytobrushes from CIN patients and analyzed by FACS analysis. Comparisons were made between populations of cervical Tregs and PD-1+ CD4+ T cells in CIN regressors and non-regressors.

Results
A median of 11% of cervical CD4+ T cells were Tregs, while a median of 30% were PD-1+ cells. The proportions of cervical CD4+ T cells that were Tregs and/or PD-1+ cells were significantly lower in CIN regressors when compared with non-regressors.

Conclusions
The prevalence of cervical tolerogenic T cells correlates inversely with spontaneous regression of CIN. Cervical Tregs may play an important role in HPV-related neoplastic immunoevasion.

Introduction

HPV infection is a major cause of cervical cancer and its precursor lesion, cervical intraepithelial neoplasia (CIN). Natural history studies of CIN[1,2] show that most infections and most CIN lesions resolve spontaneously; only a minority persists and progress to cervical cancer. Studies showing that HIV-infected women and patients who are under treatment with immunosuppressive agents have an increased incidence of CIN lesions[3,4] suggest that cell-mediated immune response against HPV viral protein is important in the control of HPV infection and progression to CIN. We have previously reported that the presence of gut-derived effector lymphocytes within the cervix plays an important role in local cell-mediated

immune responses and correlates with CIN regression.[5] The presence of robust local tolerogenic cervical T-cell responses to HPV-related neoplastic lesions would be predicted to attenuate the effects of these local effector responses. We hypothesized that the proportion of tolerogenic lymphocytes among the CD4+ T cells in the cervix would decrease among women experiencing CIN regression, thereby allowing full effect of the changes previously seen among local effector cells.

It has been reported that CD4+CD25+Foxp3+ regulatory T cells (Tregs) play an important role in tumor-associated immunoevasion in cancers (ovarian, uterine cervical, endometrial, lung, breast, pancreas, renal cell, and thyroid cancers) as well as in other proliferative disorders such as melanoma and hepatoma.[6–15] Mechanisms underlying Treg suppressive functions have been abundantly reported. The high expression of CD25 (IL-2R) on Tregs has been thought to result in cytokine deprivation-induced apoptosis of effector T cells.[16] IL-10, TGF-β, and IL-35 are also important mediators of Treg suppressive function.[16] Tregs have been reported to suppress T effectors by ligating T-effector-expressed CD80, thereby inhibiting T-cell proliferation and cytokine production. Tregs kill effector T cells, other antigen-presenting cells, and NK cells in a manner dependent on granzyme and perforin.[16]

Natural Treg cells (nTregs) differentiate in the thymus and migrate to peripheral tissues while adaptive/induced Treg cells (iTregs) differentiate in secondary lymphoid organs and tissues including mucosa-associated lymphoid tissues (MALT).[17] iTregs play essential roles in mucosal tolerance, in the control of severe chronic allergic inflammation, in the prevention of parasite and other microorganism clearance, and in the obstruction of tumor immunosurveillance while nTregs have roles in preventing autoimmunity and preventing exaggerated immune responses. iTregs appear in the mesenteric lymph nodes during induction of oral tolerance, differentiate in the lamina propria of the gut in response to microbial signals, and are generated in chronically inflamed tissues. At a minimum, Foxp3+ iTreg development requires TCR stimulation and the cytokines TGF-β and IL-2. Integrin αEβ7+ dendritic cells (DCs) residing in the MALT produce both TGF-β and retinoic acid (RA), which mediate the differentiation of naïve T cells into Foxp3+ iTregs.[17]

The programmed cell death-1 (PD-1) and PD-ligand (PD-L) pathway is also critical in the suppression of immune responses. PD-1 is a molecule inducibly expressed on peripheral CD4+ and CD8+ T cells, NKT cells, B cells, monocytes, and some DC subsets when these cells are activated by antigen receptor signaling and cytokines.[16] nTregs and iTregs can express PD-1 and PD-L1, and the expression of ligand and receptor on the same cell conveys interesting implications. Engagement of PD-1 by its ligands during T-cell receptor (TCR) signaling results in two possible T-cell responses: 1) a diminution in T-effector responses and 2) an augmentation in differentiation of naïve T cells into Foxp3+ iTreg in a TGF-β-dependent manner.[16] There are synergistic effects between the PD-1/PD-L1 pathway and TGF-β in promoting Treg development. PD-L1 is expressed on a wide variety of tumors, and high levels of PD-L1 expression strongly correlate with unfavorable prognosis in a number of cancers.[18] To this point, ligation of PD-1 may induce and maintain iTregs within the tumor microenvironment, enhance the suppression of anti-tumor T-cell responses, and thereby allow tumor progression.

Several previous studies have shown that the prevalence of Tregs among PBMCs increases in CIN patients when compared with healthy controls.[19,20] These studies assess populations of circulating Tregs using flow cytometry. Characterization of the local lymphocytes residing in cervical lesions should better reflect local immune responses to pathogen. While Nakamura et al.[21] used Foxp3 immunostaining of human CIN lesions to report the number of local Foxp3+ cells residing in the CIN lesions by immunostaining of the tissues for Foxp3 and report that the number of Foxp3-immunoreactive cells is higher in CIN3 lesions than normal or CIN1-2 lesions, no studies have quantitatively assessed populations of local Tregs, likely iTregs, in the CIN lesions using flow cytometry. Possible associations between iTregs and the natural course of CIN have also never been studied.

We have previously characterized cervical lymphocytes collected from CIN lesions using a cytobrush and have demonstrated that the majority of cervical lymphocytes in these lesions are CD3+ T cells (median 74%) and that half of the cervical CD3 + T cells are CD4+ (median 54%).[5] In the present investigations, we have analyzed the relative proportions of two tolerogenic T-cell subsets, CD25+Foxp3+ Tregs and PD-1+ T cells, among cervical CD4+ T cells collected from CIN lesions. To determine whether there was a correlation between the frequency of cervical tolerogenic T cell and the natural course of

CIN, comparisons were made between tolerogenic T-cell subsets in the lesions of CIN regressors and non-regressors.

Materials and methods

Study Population

Cervical cell samples were collected using a cytobrush from 24 patients under observation after being diagnosed with CIN by colposcopically directed biopsy. All women gave written informed consent, and the Research Ethics Committee of the University of Tokyo approved all aspects of the study. Patients with known, symptomatic or macroscopically visible vaginal inflammation, or sexually transmitted infections were excluded from our study. To study the association between cervical tolerogenic lymphocytes and CIN progression, CIN patients with regression of cervical cytology (cases) were matched with control patients who did not exhibit cytologic regression over the same time period (measured from initial detection of abnormal cytology). In this study, cytological regression was defined as normal cytology at two or more consecutive evaluations conducted at 3–4 months intervals. For the comparison of CD4+CD25+Foxp3 Tregs and PD1+CD4+ cells, 12 patients were enrolled in the regression group, and the median follow-up duration was 16.5 (8–33) months. Twelve pairs of follow-up time-matched patients with persistent cytological abnormalities were enrolled in the non-regression group, and the median follow-up time was 19 (9–34) months. Patients were interviewed about their smoking history and their last menstrual period.

Collection and Processing of Cervical Lymphocytes

Cervical cells were collected using a Digene cytobrush as described previously.[5] The cytobrush was inserted into the cervical os and rotated several times. The cytobrush was immediately placed in a 15-mL tube containing R10 media (RPMI-1640 medium, supplemented with 10% fetal calf serum, 100 mg/mL streptomycin, and 2.5 μg/mL amphotericin B) and an anticoagulant (0.1 IU/mL of heparin and 8 nM EDTA). After incubating the sample with 5 mM DL-dithiothreitol at 37 °C for 15 min with shaking, the cytobrush was removed. The tube was then centrifuged at 330 *g* for 4 min. The resulting pellet was resuspended in 10 mL of 40% Percoll. This mixture was layered onto 70% Percoll and centrifuged at 480 *g* for 18 min. The mononuclear cells at the Percoll interface were removed and washed with PBS. Cell viability was greater than 95%, as confirmed by trypan blue exclusion, and fresh samples were immediately used for further analyses.

Immunolabeling and Flow Cytometry

Cervical immune cell preparations were immunolabeled with fluorochrome-conjugated mouse monoclonal antibodies specific for the following human leukocyte surface antigens: a programmed death-1 marker (FITC–anti-PD-1), a phycoerythrin cyanine 5.5 (PC5.5)-conjugated helper T-cell marker (PC5.5–anti-CD4), and an allophycocyanin (APC)-conjugated IL-2 receptor marker (APC–anti-CD25). After exposure to primary surface-labeling antibodies, cells were washed twice with FACS buffer (10% fetal calf serum, 1 mM EDTA, 10 mM NaN3), permeabilized with Foxp3 Fixation/Permeabilization working solution (eBioscience, San Diego, CA, USA), and immunolabeled with the anti-intracellular antigen antibody, phycoerythrin (PE)-conjugated anti-Foxp3 marker (PE–anti-Foxp3). Cells were then washed twice with Flow Cytometry Staining Buffer (eBioscience) and resuspended in Flow Cytometry Staining Buffer. Additional aliquots of the cell preparations were labeled in parallel with appropriate isotype control antibodies. Antibodies were purchased from eBioscience and BD (Franklin Lakes, NJ, USA). Data were acquired using four-color flow cytometry on FACSCalibar (Becton-Dickinson, Texarkana, TX, USA). A minimum of 5000 CD4+ T cells was analyzed per sample. The position of CD4+ T cells was determined by CD4 vs SSC gating. We used KALUZA® Flow Analysis Software (Becman Coulter, Brea, CA, USA) for data analysis.

HPV Genotyping

DNA was extracted from cervical smear samples using the DNeasy Blood Mini Kit (Qiagen, Crawley, UK). HPV genotyping was performed using the PGMY-CHUV assay method.[22] Briefly, standard PCR was conducted using the PGMY09/11 L1 consensus primer set and human leukocyte antigen-DQ (HLA-DQ) primer sets. Reverse blotting hybridization was performed. Heat-denatured PCR amplicons were hybridized to specific probes for 32 HPV genotypes

and HLA-DQ reference samples. The virological background (HPV genotyping) of 24 patients in our study is shown in Table I. HPVs 16, 18, 31, 33, 35, 39, 45, 51, 52, 53, 56, 58, 59, 68, 73, and 82 were defined as high-risk HPVs according to an International Agency for Research on Cancer (IARC) multicenter study.[23]

Statistical Analysis

Statistical analyses, including calculation of medians and interquartile ranges (IQRs), were performed using the commercial statistical software package JMP® (SAS, Cary, NC, USA). Wilcoxon rank sum tests or Fisher's exact tests were applied for matched pair comparisons. *P*-values ≤ 0.05 were considered significant.

Results

Isolation of Cervical Tolerogenic T-cell Subsets in CIN Lesions

To assess cervical tolerogenic T cells, cervical samples were collected from CIN lesions positive for any HPV genotype and fractionated over a discontinuous Percoll density gradient to remove cervical epithelial cells. Cervical lymphocytes were then isolated from the interphase between Percoll and culture medium.[5] Cervical CD4+ T cells were identified among the isolated lymphocytes using CD4 vs SSC gating. The percentages of CD4+ cervical T cells that were CD25+Foxp3+ Tregs or that were PD-1+ were determined by flow cytometry. Two representative cases are displayed in Fig. 1(a,b), respectively. The proportion of cervical CD4+ T cells that were CD25+Foxp3+ was 14.2% whereas the proportion of CD4+ T cells that displayed PD-1 was 33.6% (bold lines). Among all CIN patients, a median of 11.7% (IQR: 7.3–14.6, $n = 24$) of CD4+ cervical T cells were CD25+Foxp3+ Tregs, while a median of 30.7% (20.2–38.5, $n = 24$) of CD4+ cells expressed PD-1. The proportions of tolerogenic T-cell subsets found in cervical preparations were markedly higher than those reported in circulating peripheral blood where approximately 5% of PBMCs are CD25+Foxp3+ Tregs[24] and 5% of peripheral CD4+ T cells are PD-1+.[25] These data indicate that the cervical mucosal T cells separation technique used for these investigations isolated a population of T cells with characteristics that suggest little to no contamination by peripheral blood. Further, should small amounts of contamination occur during isolation the effect on overall results would be predicted to be minimal.

Table I Patients infected with multiple HPV types were included.

HPV type	Total numbers (%)
16	5 (16.6)
18	2 (6.6)
31	1 (3.3)
45	1 (3.3)
51	1 (3.3)
52	3 (10)
53	3 (10)
55	3 (10)
56	4 (13.3)
58	5 (16.6)
70	2 (6.6)
Total	30 (100)

Of 24 patients, 4 (16.6%) were infected with multiple types. HPVs 16, 18, 31, 33, 35, 39, 45, 51, 52, 53, 56, 58, 59, 68, 73, and 82 were defined as high-risk HPVs.

Correlation of Cervical Tregs and PD-1+ CD4+ cells in CIN Lesions with Menstrual Phase, HPV Types, Smoking History, and CIN Course

Many factors, including HPV genotypes, smoking, and other microbial infections, have been reported to associate with spontaneous regression or progression of CIN.[26] In this study, we obtained cervical Tregs from histologically diagnosed CIN patients and sought correlations between cervical Tregs and potential clinical factors, which may associate with the natural course of CIN. Patients with known, symptomatic or macroscopically visible vaginal inflammation, or sexually transmitted infections other than HPV were excluded from our study. All patients were diagnosed with CIN1-2 at the time of enrollment and followed with colposcopy and cervical cytology smears every 4 months.

To account for possible confounding factors, samples from our 24 CIN patients were reanalyzed after segregation by each of the following characteristics: menstrual phase (proliferative vs secretory), HPV genotype (high risk vs low risk), and smoking history (smoking vs non-smoking). The prevalence of CD25+Foxp3+ Tregs and of PD-1+ T cells among cervical CD4+ cells was compared between each of the

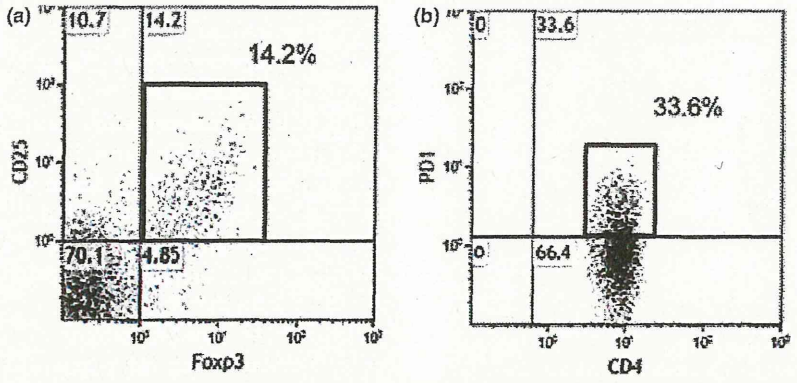

Fig. 1 Representatives of flow cytometric analysis of immune cells isolated from cervical intraepithelial neoplasia lesions. Bold lines delimit cervical CD4+CD25+Foxp3+ Tregs (a) and PD1+ CD4+ T cells (b). The indicated percentages represent percentage of total CD4+ T cells.

two groups using Wilcoxon rank sum testing (Table II). None of these possible confounders correlated with CD25+Foxp3+ Tregs and PD-1+ T cells results in CIN lesions, indicating that the tolerogenic T cells residing in the cervical mucosa were not influenced by smoking, hormonal status, or infecting HPV subtypes.

Next, we compared populations of CD25+Foxp3+ Tregs and PD-1+ T cells residing in the CIN lesions of regressors ($n = 12$) and non-regressors ($n = 12$) to determine whether there was an association between the frequency of cervical tolerogenic T-cell subsets and spontaneous regression of CIN. Twelve patients had spontaneous regression of their CIN lesions, and these women had a median follow-up duration of 16.5 (8–33) months. The non-regression group consisted of twelve women with persistent cytological abnormalities who were matched to the spontaneous regressor cohort by follow-up time. No significant differences were seen in the detection rates of high-risk HPV (58.3% vs 83.3%, $P = 0.37$), percent of CIN 2 at the enrollment (33.3% vs 58.3%, $P = 0.4$), and the median ages (33 years old vs 36, $P = 0.44$) of patients in the regression and non-regression groups. Among regressors, cervical CD25+Foxp3+ Tregs comprised a median of 7.3% (IQR: 6.3–11.4) of cervical CD4+ cells; the rate among non-regressors was 13.9% (IQR: 11.6–16.9). The frequency of cervical CD25+Foxp3+ Tregs in regressors was significantly lower than that in non-regressors ($P = 0.0012$) (Table II and Fig. 2). Similarly, cervical PD1+ CD4+ cells comprised a median of 20.8% (IQR: 15.8–31.9) of cervical CD4+ cells among regressors whereas a median of 35.1% (IQR:

Table II Correlation of the proportions of cervical Treg and PD-1+ cells among cervical CD4+ T-cell populations with clinical characteristics

		Percentage of total cervical CD4+ T cells			
Factors	Groups	CD25+Foxp3+ Tregs		PD-1+ cells	
Menstrual phase	Proliferative	10.26 (7.04–15.4)	$P = 0.94$	29.8 (22.7–39.5)	$P = 0.72$
	Secretory	12.0 (7.1–14.2)		28.1 (18.9–36.7)	
HPV genotype	High risk	11.8 (7.8–14.2)	$P = 0.67$	29.8 (20.3–38.2)	$P = 0.82$
	Low risk	7.4 (6.7–15.7)		33.5 (18.5–45.4)	
Smoking	Smoking	10.2 (7.3–14.7)	$P = 0.73$	29.8 (19.5–39.5)	$P = 0.80$
	Non-smoking	10.8 (5.0–15.9)		24.6 (19.6–40.9)	
CIN course	Regression	7.3 (6.3–11.4)	$P = 0.0012$	20.8 (15.8–31.9)	$P = 0.018$
	Non-regression	13.9 (11.6–16.9)		35.1 (30.2–42.6)	

Association of cervical CD4+CD25+Foxp3+ Tregs and PD1+CD4+ cells with menstrual cycle, HPV genotype, smoking, and cervical intraepithelial neoplasia (CIN) course were shown.

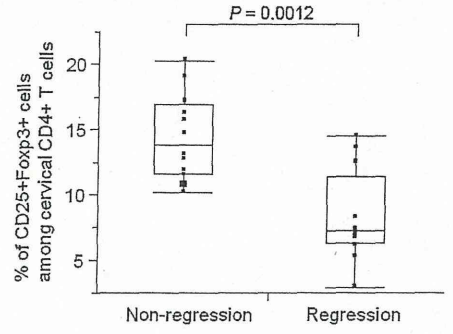

Fig. 2 Association of cervical Tregs with the natural course of cervical intraepithelial neoplasia. Among regressors, cervical Tregs comprised a median of 7.33% [Interquartile ranges (IQR): 6.38–11.4, $n = 12$] of CD4+ cervical T cells; the rate among non-regressors was 13.9% (IQR: 11.6–16.9, $n = 12$); $P = 0.0012$.

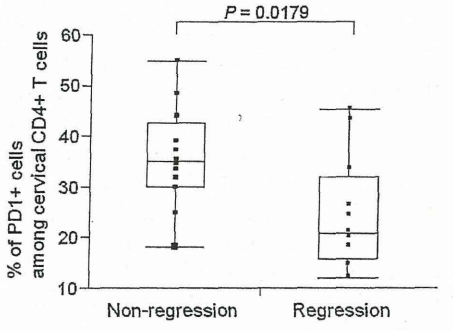

Fig. 3 Association of cervical PD-1+ CD4+ T cells with the natural course of cervical intraepithelial neoplasia. Among regressors, cervical PD1+ cells comprised a median of 20.8% [Interquartile ranges (IQR): 15.8–31.9, $n = 12$] of CD4+ cervical T cells; the rate among non-regressors was 35.1% (IQR: 30.2–42.6, $n = 12$); $P = 0.0179$.

30.2–42.6) among non-regressors. Again, the frequency of cervical PD-1+ CD4+ cells in regressors was significantly lower than that in non-regressors ($P = 0.017$) (Table II and Fig. 3).

Discussion

Although many studies have been reported about the positive association between tolerogenic lymphocytes and poor prognosis in many cancers, there are limited data on similar associations in women with HPV-related cervical precursor lesions. Our results show that the prevalence of CD25+ Foxp3+ Tregs and of PD1+ CD4+ T cells residing in cervical precursor lesions inversely correlates with spontaneous regression of CIN.

The peripheral population of Foxp3+ Tregs includes nTregs and iTregs. iTregs play essential roles in mucosal tolerance, in the control of severe chronic allergic inflammation, and in the prevention of organism clearance and tumor immunosurveillance, while nTregs have roles in preventing autoimmunity and exaggerated immune responses.[17] We would predict that the majority of cervical CD25+Foxp3+ Tregs assessed in this study are iTregs although definitive isolation of iTregs is hampered by the lack of suitable surface markers that distinguish iTreg and nTreg cell populations.

In this study, cervical Treg prevalence negatively correlated with regression of CIN (Fig. 2) but did not correlate with CIN grade (data not shown). Supporting our data, several previous studies have shown a positive correlation between Treg prevalence in peripheral blood and high grade of CIN.[19,20] Of course, cervical iTregs and circulating Tregs may differ in their TCR repertoire. iTregs are known to differentiate from mature naïve CD4+ cells through the effects of TGF-β and RA secreted by mucosa-associated DCs.[17] In our data, the proportion of CD25+Foxp3+ Tregs among total cervical CD4+ cells (a median of 11%) was twofold higher than previously reported peripheral blood levels (approximately 5%). This suggests that iTregs may be generated continuously, probably in an antigen-depending manner, and accumulate in chronically HPV-infected tissues and CIN lesions. Others have reported that Foxp3 mRNA levels in cervical samples that included exfoliated epithelial cells and cervical lymphocytes are higher among high-grade squamous intraepithelial lesion (HSIL) patients when compared with low-grade squamous intraepithelial lesion (LSIL) patients.[27] However, it is unknown whether Foxp3 mRNA levels in these cervical samples parallel the number of Tregs because cervical lymphocytes were not specifically isolated in this study.

Although the persistence of HPV infection was not followed in the present study, Molling et al.[20] reported that CD4+CD25hi Treg frequency correlates with persistence of HPV type 16. Tregs may inhibit the HPV clearance by immune cells such as invariant natural killer T cells.

TGF-β is critical to the induction and maintenance of Foxp3+ Tregs, with particular importance in the induction of iTregs from naive T cells and in the conversion of effector T cells to iTregs. Several studies have demonstrated that the expression of TGF-β and RA receptors in cervical specimens is lower in

CIN lesions when compared with normal epithelium.[28,29] In these studies, there was no correlation between TGF-β mRNA levels and either CIN grade or CIN natural course. TGF-β-induced iTreg frequency may be a more direct predictor of CIN progression than TGF-β. In fact, measurement of tolerogenic T-cell frequency in CIN lesions has the potential to prove useful in determining individualized screening and treatment paradigms.

Whether sex hormones modulate the prevalence and function of Tregs remains controversial. Arruvito et al. reported that the proportion of Foxp3+ cells within the peripheral blood CD4+ T-cell population increases during the late follicular phase when compared with the luteal phase.[29] The expansion of Tregs during the follicular phase was highly correlated with serum estradiol (E2) levels.[30] In contrast, Weinberg et al. reported recently that there are no significant correlations between changes in serum E2 levels and the prevalence of any circulating Treg subtypes or between changes in serum progesterone levels and the proportion of CD8+ Foxp3+ Tregs in peripheral blood samples.[31] The effect of smoking on the generation of tolerogenic T cells is also controversial.[32–34] Note that all of the above studies assess peripheral circulating rather than local cervical Tregs. Our data on the latter cells revealed no correlations between cervical Treg prevalence and either menstrual phase or smoking.

In this study, we focused on PD-1+ CD4+ T cells as well as Foxp3+ Tregs as engagement of PD-1 by its ligands on T cells is critical to the differentiation of naïve T cell into Foxp3+ iTregs. Furthermore, Tregs and the PD-1/PD-L pathway are integral in terminating immune responses and augmenting the suppression of anti-tumor T-cell responses. In short, the PD-1 pathway controls the development, maintenance, and function of iTregs at mucosal sites. Here, we show that PD-1+ T cells are more frequently found among cervical T cells than among PBMCs and that the prevalence of PD1+ T cells in CIN lesions (likely reflecting cervical iTregs) correlates inversely with spontaneous regression of CIN. Assessment for other tolerogenic T-cell subsets (e.g., Foxp3-IL10+ Tr1, Foxp3-TGF-β+ Th3) in this study, while potentially informative, was limited by the number of cervical lymphocytes that could be isolated from a single cytobrush sample.

In summary, even the study population is small and the results are limited, our flow cytometric analyses demonstrate for the first time that a prevalence of CD4+ CD25+ Foxp3+ Tregs infiltrating into CIN lesions significantly correlates with regression of CIN regardless of HPV subtype. Conversely, a high prevalence of lesional cervical Tregs may be responsible for CIN persistence as well as HPV infections and might function as a useful predictive biomarker for progression of CIN.

Acknowledgements

We thank Dr. Ai Tachikawa-Kawana for expert advice about flow cytometry. This work was supported by a grant from the Ministry of Health, Labour and Welfare of Japan for the Third-Term Comprehensive Strategy for Cancer Control and for Comprehensive Strategy for Practical Medical Technology and by a grant from the Ministry of Education, Culture, Sports, Science and Technology of Japan and by a grant from Tokyo IGAKUKAI.

References

1 Holowaty P, Miller AB, Rohan T, To T: Natural history of dysplasia of the uterine cervix. *J Natl Cancer Inst* 1999; 91:252–258.
2 Moscicki AB, Schiffman M, Kjaer S, Villa LL: Chapter 5: updating the natural history of HPV and anogenital cancer. *Vaccine* 2006; 24:42–51.
3 Ellerbrock TV, Chiasson MA, Bush TJ, Sun XW, Sawo D, Brudney K, Wright TC Jr: Incidence of cervical squamous intraepithelial lesions in HIV-infected women. *JAMA* 2000; 283:1031–1037.
4 Ognenovski VM, Marder W, Somers EC, Johnston CM, Farrehi JG, Selvaggi SM, McCune WJ: Increased incidence of cervical intraepithelial neoplasia in women with systemic lupus erythematosus treated with intravenous cyclophosphamide. *J Rheumatol* 2004; 31:1763–1767.
5 Kojima S, Kawanna K, Fujii T, Yokoyama T, Miura S, Tomio K, Tomio A, Yamashita A, Adachi K, Sato H, Nagamatsu T, Schust DJ, Kozuma S, Taketani Y: Characterization of Gut-Derived Intraepithelial Lymphocyte (IEL) Residing in Human Papillomavirus (HPV)-Infected Intraepithelial Neoplastic Lesions. *Am J Reprod Immunol* 2011; 66:435–443.
6 Wolf D, Wolf AM, Rumpold H, Fiegl H, Zeimet AG, Muller-Holzner E, Deibl M, Gastl G, Gunsilius E, Marth C: The expression of the regulatory T cell-specific forkhead box transcription factor FoxP3 is associated with poor prognosis in ovarian cancer. *Clin Cancer Res* 2005; 11:8326–8331.
7 Jordanova ES, Gorter A, Ayachi O, Prins F, Durrant LG, Kenter GG, van der Burg SH, Fleuren GJ: Human leukocyte antigen class I, MHC class I chain-related molecule A, and CD8+/regulatory T-cell ratio: which variable determines survival of cervical cancer patients? *Clin Cancer Res* 2008; 14:2028–2035.
8 Yamagami W, Susumu N, Tanaka H, Hirasawa A, Banno K, Suzuki N, Tsuda H, Tsukazaki K, Aoki D: Immunofluorescence-detected infiltration of CD4+FOXP3+ regulatory T cells is relevant to the prognosis of patients with endometrial cancer. *Int J Gynecol Cancer* 2011; 21:1628–1634.